



HAL
open science

Investigating the Role of Cobalt(II) in the Single-Molecule Magnets Behavior of 2p-3d-4f clusters

Ghénadie Novitchi, Sergiu Shova, Cyrille Train

► **To cite this version:**

Ghénadie Novitchi, Sergiu Shova, Cyrille Train. Investigating the Role of Cobalt(II) in the Single-Molecule Magnets Behavior of 2p-3d-4f clusters. *Inorganic Chemistry*, 2022, 61 (43), pp.17037-17048. 10.1021/acs.inorgchem.2c01742 . hal-03817520

HAL Id: hal-03817520

<https://hal.science/hal-03817520v1>

Submitted on 17 Oct 2022

HAL is a multi-disciplinary open access archive for the deposit and dissemination of scientific research documents, whether they are published or not. The documents may come from teaching and research institutions in France or abroad, or from public or private research centers.

L'archive ouverte pluridisciplinaire **HAL**, est destinée au dépôt et à la diffusion de documents scientifiques de niveau recherche, publiés ou non, émanant des établissements d'enseignement et de recherche français ou étrangers, des laboratoires publics ou privés.

Investigating the Role of Cobalt(II) in the Single-Molecule Magnets Behavior of 2p-3d-4f clusters.

Ghénadie Novitchi,[†] Sergiu Shova,[‡] and Cyrille Train*,[†]

[†] Laboratoire National des Champs Magnétiques Intenses (LNCMI)

Univ. Grenoble Alpes, INSA Toulouse, Univ. Toulouse Paul Sabatier, EMFL, CNRS
F-38042 Grenoble, France

[‡]“Petru Poni” Institute of Macromolecular Chemistry, Aleea Gr. Ghica Voda 41A, 700487 Iasi, Romania

Abstract

1,5-dimethyl-3-(3'-(hydroxymethyl)-2'-pyridine)-6-oxotetrazane ($H_3vdpyCH_2OH$) or its oxidized verdazyl form ($vdpyCH_2OH$) are reacted with transition metal and/or lanthanide acetates to yield $[(vdpyCH_2O)_2Co_2Ln_2(acO)_8]$ ($Ln=Y(III): I_{Co,Y}; Gd(III): I_{Co,Gd}$), $[(vdpyCH_2O)_2M_3(acO)_4]$ ($M=Zn(II): II_{Zn}; Co(II): II_{Co}$) and $[(vdpyCH_2OH)Zn(acO)_2]$ (III_{Zn}) through self-assembly implying a complex-as-ligand intermediate. Single-crystal diffraction reveals that $I_{MT,Ln}$ are composed of 2p-3d-4f centrosymmetric clusters with verdazyl radicals at the two ends coordinated to the transition metal ion in a tridentate mode and to the $\{Ln_2(acO)_4\}$ lanthanide central core in a monodentate mode through its alkoxo moiety. In $I_{Co,Gd}$, the transition metal ions adopt an irregular octahedral environment and the $\{Ln_2(acO)_4\}$ core a paddlewheel motif whereas in $I_{Co,Y}$, the transition metal is pentacoordinated and the central core contains only two acetate bridges. Going from $I_{Co,Y}$ to II_{Co} , the central $\{Y_2(acO)_4\}$ core is replaced by an axially compressed octahedral cobalt(II) center whereas the outer parts of the molecule remain still. The *dc* magnetic studies revealed that the alternate π -stacking of the verdazyl radicals in II_{Zn} led to the formation of alternate antiferromagnetically coupled 1D chains with $J_{vd-vd} = -8.2(1) \text{ cm}^{-1}$ and $J_{vd-vd}' = -7.6(1) \text{ cm}^{-1}$ ($H = -2JS_1.S_2$). In $I_{Co,Y}$, a complex fitting procedure allowed to retrieve a complete set of magnetic parameters to take into account both the magnetic anisotropy of the cobalt(II) centers and intra- and inter-molecular exchange effects. For $I_{Co,Y}$, it led to $g_{Co} = 2.13(4)$, $D_{Co} = 100(2) \text{ cm}^{-1}$, $E_{Co} = 19.9(5) \text{ cm}^{-1}$, $J_{Co-vd} = +26.5(4) \text{ cm}^{-1}$ and $J_{vd-vd} = -7.95(4) \text{ cm}^{-1}$. *ac* magnetic susceptibility of $I_{Co,Y}$, $I_{Co,Gd}$ and II_{Co} did not reveal any slow relaxation of the magnetization even when a *dc* external magnetic field up to 2000 Oe was applied.

Introduction

The slow relaxation of the magnetization in discrete coordination clusters or complexes has been an active field of research since its discovery in $Mn_{12}O_{12}(O_2CCH_3)_{16}$.¹ It has been possible to identify that the key parameter for the observation of a single molecule-magnet (SMM) behavior was the magnetic anisotropy of the paramagnetic ions leading to the study of smaller clusters and, ultimately, of single-ion magnets. In general, the system contains essentially one anisotropic metal ions like $Mn(III)$ ¹ $Co(II)$ ^{2,3,4,4,5,6,7} or $Ln(III)$ ^{8,9,10,11}. Nonetheless, in order to increase the anisotropy barrier to be overcome to flip the magnetization, synthetic chemists have tentatively combined several anisotropic ions.^{12,13,14} In a recent communication, we have followed this strategy and synthesized a hetero-tri-spin 2p-3d-4f discrete cluster of formula $[(vdpyCH_2O)_2Co_2Dy_2(acO)_8]$ ($vdpyCH_2O = 1,5\text{-dimethyl-3-(2'-(5-hydroxymethylpyridyl))-6-oxoverdazyl}$; $acOH = CH_3COOH$) that exhibits SMM properties.¹⁵ Two anisotropic ions, namely $Co(II)$ and $Dy(III)$, are present in this cluster. It is thus difficult to figure out whether

the SMM behavior arises from the presence of either of the two metal ions and/or from a synergy between the two anisotropic spin bearers. The most natural way for synthetic chemists to unravel the respective role of these metal ions is to perform chemical substitutions onto the parent compound and/or to study “simpler” though comparable systems. The two approaches are followed in the present case to underline the role of the cobalt(II) ion in the magnetization relaxation: the substitution onto the two lanthanide sites of $[(\text{vdpyCH}_2\text{O})_2\text{Co}_2\text{Dy}_2(\text{acO})_8]$ ($\mathbf{I}_{\text{Co,Dy}}$) yielded $[(\text{vdpyCH}_2\text{O})_2\text{Co}_2\text{Ln}_2(\text{acO})_8]$ ($\text{Ln}=\text{Y(III)}: \mathbf{I}_{\text{Co,Y}}; \text{Gd(III)}: \mathbf{I}_{\text{Co,Gd}}$) whereas two simpler clusters of formula $[(\text{vdpyCH}_2\text{O})_2\text{M}_3(\text{acO})_4]$ ($\text{M}=\text{Zn(II)}: \mathbf{II}_{\text{Zn}}; \text{Co(II)}: \mathbf{II}_{\text{Co}}$) were obtained. For the former series, a particular attention is paid to the subtle structural variations occurring during the substitutions of the lanthanide ion together with the changes in the static and dynamic magnetic properties provoked by these substitutions. The latter, together with the mononuclear zinc complex $[(\text{vdpyCH}_2\text{OH})\text{Zn}(\text{acO})_2]$ (\mathbf{III}_{Zn}) bring valuable magnetic information but also important insights about the processes at work during the self-assembly of the 2p-3d-4f clusters.

Results and Discussion

Synthesis

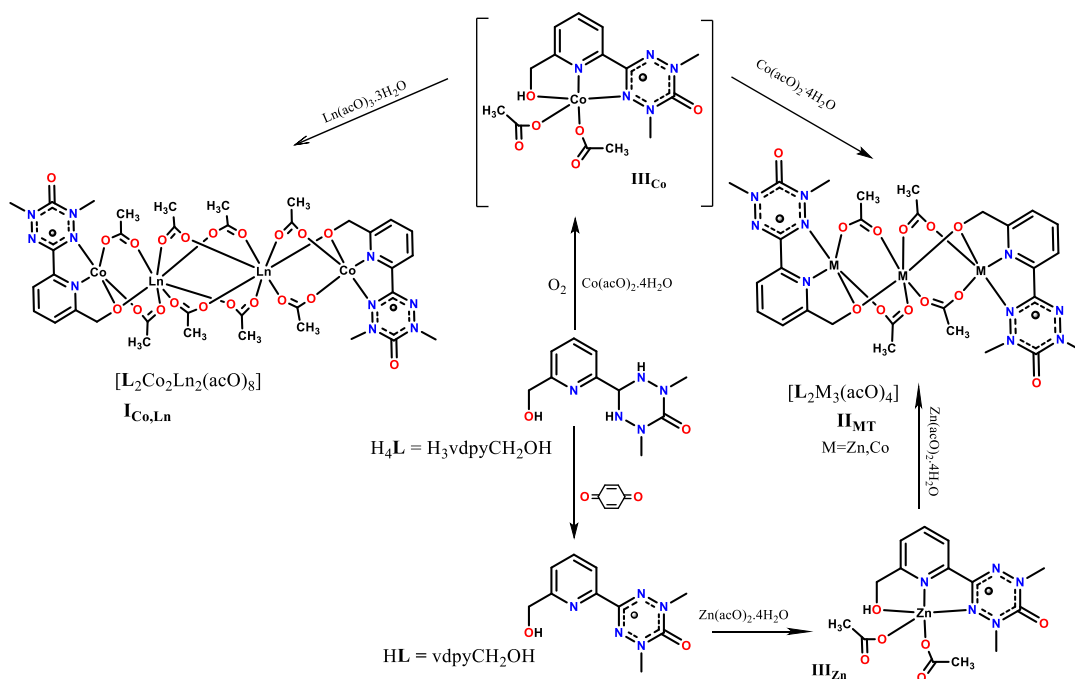


Figure 1. Reaction scheme of chemical transformation with tetrazane ($\text{H}_3\text{vdpyCH}_2\text{OH}$) and verdazyl radical (vdpyCH_2OH) towards heterospin clusters.

The synthesis of these two series of coordination compounds begins with the synthesis and purification of the tetrazane precursor (H_4L). It is a well described two-step procedure, the key step being the condensation of the *bis*(1-methylhydrazide)carbonic acid and 6-(hydroxymethyl)-2-pyridinecarbaldehyde. The resulting tetrazane is purified by recrystallization in dichloromethane or methanol yielding two isomorphs of the molecule as revealed by single crystal X-ray diffraction. As described in our preliminary work, the synthesis

of [(vdpyCH₂O)₂Co₂Dy₂(acO)₈] was undertaken using a one-pot method starting from 1,5-dimethyl-3-(2'-(5-hydroxymethyl)pyridyl)-6-oxotetrazane and the two metal acetates (Figure 1 upper left route).¹⁵ The self-assembly process leading to the cluster proceeds through an autocatalytic oxidation of the tetrazane moiety into a verdazyl radical. As previously demonstrated,^{16–18,19} this oxidation is definitely favored by the presence of redox-active transition metal ions like cobalt(II). Accordingly, we used this strategy to substitute the lanthanide(III) ion present in the cluster and obtain [(vdpyCH₂O)₂Co₂Ln₂(acO)₈] (Ln=Y(III): **I**_{Co,Y}; Gd(III): **I**_{Co,Gd}). The advantage of this technique is that the gradual oxidation of the tetrazane is compatible with the kinetics of crystallization, affording the compounds essentially as single crystals.

This also holds for the synthesis of compounds where only the transition metal ion is present: **II**_{Co} is obtained as single crystals through a one-pot synthesis in air starting from equimolar ratio of tetrazane and cobalt(II) acetate (Figure 1 upper right route). When such redox-active partners, e.g. for all the zinc(II) derivatives, are not present, it is necessary to oxidize the organic precursor prior to complexation. Several oxidants were used in the literature depending on the nature of the tetrazane substituents. In the present case, we used the benzoquinone route initially proposed by Hicks and coll.²⁰ because of the solubility of the tetrazane in most organic solvents and the good stability of the adduct obtained during the oxidation.^{21,22} The chemical stability of the free radicals is indeed an important issue in radical chemistry in general and in the verdazyl case in particular:^{23–26} some radicals are essentially stable whereas others can only be detected as intermediates of complex chemical reactions. Verdazyl radical has proven to have a relatively good stability and form stable coordination compounds.^{25,27–35} Nonetheless, this possibility is dependent upon the substituent bonded to the radical. In turn, uncoordinated pyridine-substituted verdazyl radicals are rather unstable and decompose within 2 days.^{17,20,36,37} The stability can be increased by substituting the methyl groups of the oxoverdazyl moiety by isopropyl groups but these bulky groups modify the coordination chemistry of the radical and the packing of the clusters. This strategy was thus not applicable in the present case so that the radical was prepared and purified immediately prior to complexation.³⁸ Then **II**_{Zn} was obtained as a crystalline powder by oxidizing tetrazane prior to complexation (Figure 1 lower right route).

For one-pot synthesis, the first signature of the *in situ* oxidation of the tetrazane is the gradual color change from pink to intense red during the one-hour reaction.^{16–18} For all compounds, the observation assessing the formation of the radical is the typical position of the vibration of the carbonyl group of the verdazyl radical ($\nu_{C=O} = 1681 \text{ cm}^{-1}$) observed in FTIR and its important shift ($\Delta\nu_{C=O} = 62 \text{ cm}^{-1}$) compared to that of the tetrazane precursor ($\nu_{C=O} = 1619 \text{ cm}^{-1}$) (see Figure SI-1). Moreover, a detailed analysis of the whole IR spectra indicates a close similarity for **I**_{Co,Y}, **I**_{Co,Gd}, and **I**_{Co,Dy} on one side and for **II**_{Co} and **II**_{Zn} on the other (see Figure SI-2,3) but it is difficult to attribute these changes to specific structural features. Accordingly, a complete single-crystal X-ray study was performed to assess the structural details of these two series of compounds. During the synthetic process, **III**_{Zn} is formed and crystallized as secondary product. The crystal resolution of this compound (see below) is an important input in the understanding of the self-assembly processes occurring in solution (Figure 1). It indicates that the first step of the coordination chemistry of these clusters is the complexation of the transition metal ion by the verdazyl proligand to the diacetate metal(II) complex. In a *in situ* complex-as-

ligand approach, this complex then acts as a tridentate ligand through one oxygen atom of the two acetate ligands and, upon deprotonation, through the alcoholic function of the verdazyl radical. Two of these metallo-ligands bind to the acetate-bridged dinuclear lanthanide cluster to yield the compounds of the $\mathbf{I}_{MT,Ln}$ series or to a single transition metal ion to yield those of the \mathbf{II}_{MT} series.

X-ray structures

1,5-dimethyl-3-(3'-(hydroxymethyl)-2'-pyridine)-6-oxotetrazane ($H_3vdpyCH_2OH$) recrystallized from methanol or CH_2Cl_2 shows two different FT-IR spectra (Figure SI-4). The most striking differences are in the 3100-3600 cm^{-1} frequency range, e.g. for the stretching vibrations of the NH and OH groups. In the FTIR spectra of two forms of oxotetrazane, three distinguished absorption bands can be detected. For H_4L^{MeOH} , two fine asymmetric bands appear at 3271 and 3228 cm^{-1} whereas they are located at 3242 and 3197 cm^{-1} for H_4L^{DCM} . In both cases, these two bands can be assigned to the symmetric and antisymmetric NH vibrations. A third large and intense absorption band at higher wavenumbers has its maximum shifted from 3300 cm^{-1} in H_4L^{MeOH} to 3409 cm^{-1} in H_4L^{DCM} . It is assigned to OH stretching. Upon dissolution of the crystals in DMSO or $CDCl_3$, the NMR spectra are identical for H_4L^{MeOH} and H_4L^{DCM} (Figure SI-5,6). This is a strong indication that the two forms contain identical molecules and essentially differ by the conformation and/or crystal packing comprising different H-bondings, hence modifying the OH and NH stretching energies. To refine this interpretation, let us examine the common features and the differences between the two forms revealed by the single-crystal X-ray analysis (Figure 2).

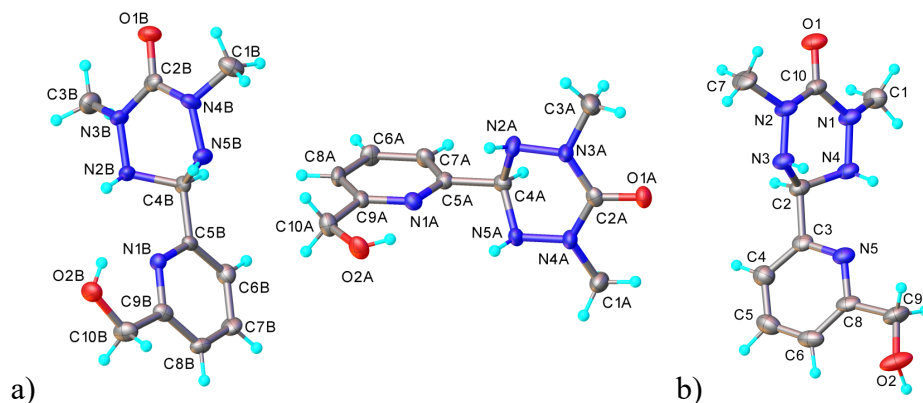


Figure 2. X-ray Molecular structures of 1,5-dimethyl-3-(3'-(hydroxymethyl)-2'-pyridine)-6-oxotetrazane ($H_3vdpyCH_2OH$), recrystallized a) from dichloromethane with two asymmetric molecules in the unit cell (H_4L^{DCM}); b) from methanol (H_4L^{MeOH}).

In both cases, the oxotetrazane ring can be easily distinguished from its oxidized form through the refinement of the hydrogen atoms located on the N2, N5 and C4 atoms of the tetrazane ring. They lead to a tetragonal geometry around these atoms and ruin out the planarity of the six-membered ring observed for oxoverdazyl.³⁹ The second common point is the relative orientation of the tetrazane ring and substituted pyridine: intramolecular H-bonds between the two NH groups of the former and the nitrogen atom of the latter leads to a nearly perpendicular orientation of the two cycles already observed with unsubstituted pyridine moieties.^{40,41} Finally,

the main difference between the two conformers is the orientation of the methylhydroxyl group (CH₂OH). When recrystallized from methanol, the hydroxyl group points outward of the molecule and is solely engaged in an intermolecular H-bond with the carbonyl group of the tetrazane ring of the neighboring molecule whereas, when recrystallized from dichloromethane, it makes an additional intramolecular H-bond with the nitrogen atom of the pyridine cycle and therefore points inwards. We can tentatively assume that this difference is reminiscent of the organization in solution, the most polar solvent (methanol) favoring the formation of a conformer with a larger dipolar moments. Let us note that the intermolecular H-bonds lead to the formation of 1D supramolecular organization with straight chains for H₄L^{MeOH} (Figure SI-7) and zig-zag ones for H₄L^{DCM} (Figure SI-8).

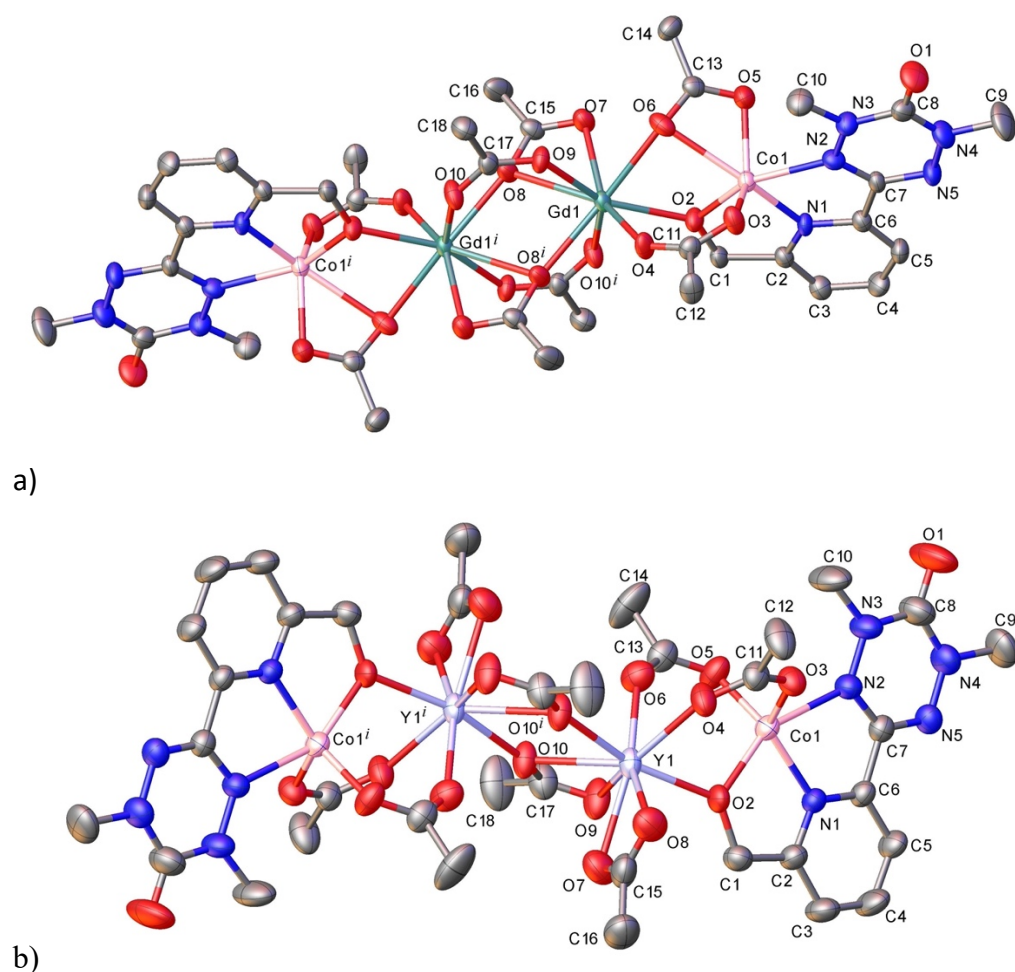


Figure 3. X-ray molecular structure of a) ICo,Gd and b) ICo,Y with atom labeling scheme and thermal ellipsoids at 30 % probability level.

Compounds ICo,Gd , and ICo,Y crystallize in the centrosymmetric $P-1$ and $P2_1/c$ space groups respectively (Table 1). Nonetheless, in both cases, the structure resolution reveals the presence of isolated centrosymmetric molecular clusters of formula $[(\text{vdpyCH}_2\text{O})_2\text{Co}_2\text{Ln}_2(\text{acO})_8]$ (Figure 3). In the three compounds, two equivalent verdazyl ligands are present at the edges of the cluster. In contrast with the situation encountered in $\text{H}_4\text{L}^{\text{MeOH}}$ and $\text{H}_4\text{L}^{\text{DCM}}$, the tetranitrogenated ring is flattened due to sp^3 to sp^2 hybridization of N2, C4 and N5 upon oxidation of the tetrazane ring. Moreover, the alkoxo group is deprotonated, allowing the radical to coordinate to the transition metal ion through the oxygen atom of

this group and the nitrogen atoms of the pyridine and verdazyl rings. The verdazyl radical thus behaves as a tridentate meridional ligand towards the transition metal ion as observed in the parent Co-Dy compounds.¹⁵ In $\mathbf{I}_{\text{Co,Gd}}$, the coordination sphere of the transition metal ions is completed by three oxygen atoms from two bridging acetates, one in a $\kappa^3\text{O},\text{O}':\text{O}'$ ($\eta^2:\eta^1:\mu_2$) coordination mode and the other in a $\kappa^2\text{O},\text{O}'$ ($\eta^1:\eta^1:\mu_2$) mode leading to an irregular six-coordinated environment where the longer distances are Co-N1 (2.275 Å), N1 being the nitrogen atom of the verdazyl ring and Co-O4 (2.395 Å), O4 being the oxygen atom of the acetate ligand also coordinated to the gadolinium(III) center. The former case is a confirmation of the rather weak Lewis basicity of the verdazyl ring and the latter is due to the simultaneous complexation of the transition metal and the lanthanide ions. The mean Co-ligand distance (2.12 Å) is typical for oxidation state +II of cobalt. In $\mathbf{I}_{\text{Co,Y}}$, the situation is slightly different since the distance between the transition metal and O4 is above 3 Å discarding the existence of a coordination bond. Accordingly, the transition metal ions are pentacoordinated and both acetate groups adopt the $\kappa^2\text{O},\text{O}'$ ($\eta^1:\eta^1:\mu_2$) mode coordination mode. In both cases, the central core of the cluster is a $\{\text{Ln}_2(\text{acO})_4\}$ unit. The atoms of the first coordination sphere of the lanthanide ions are the oxygen atom of the alkoxo group of the verdazyl ligand (O1) and two oxygen atoms of the acetate bridging with the transition metal ions (O4, O6). Then, in $\mathbf{I}_{\text{Co,Gd}}$, the coordination sphere is completed by five oxygen atoms from four acetate bridging the two gadolinium atoms, two in a $\kappa^3\text{O},\text{O}':\text{O}'$ ($\eta^2:\eta^1:\mu_2$) mode and two in a $\kappa^2\text{O},\text{O}'$ ($\eta^1:\eta^1:\mu_2$) one. The paddlewheel Gd_2 core is thus very similar to the one observed in the Co-Dy parent compound.¹⁵ The Gd...Gd distance is worth 3.9201(9) Å, slightly larger than the one observed in the Co-Dy derivatives in accordance with the reduction of the ionic radius along the lanthanide series. As for the situation of the transition metal ions, in $\mathbf{I}_{\text{Co,Y}}$, the situation of the lanthanide is slightly different since the five complementary oxygen atoms surrounding the lanthanide ions arise from one bidentate acetate and two $\kappa^3\text{O},\text{O}':\text{O}'$ ($\eta^2:\eta^1:\mu_2$) bridging ones. In these compounds, the paddlewheel motif is thus lost and this modifies the relative orientation of coordination polyhedra of the two lanthanides (Figure 4).

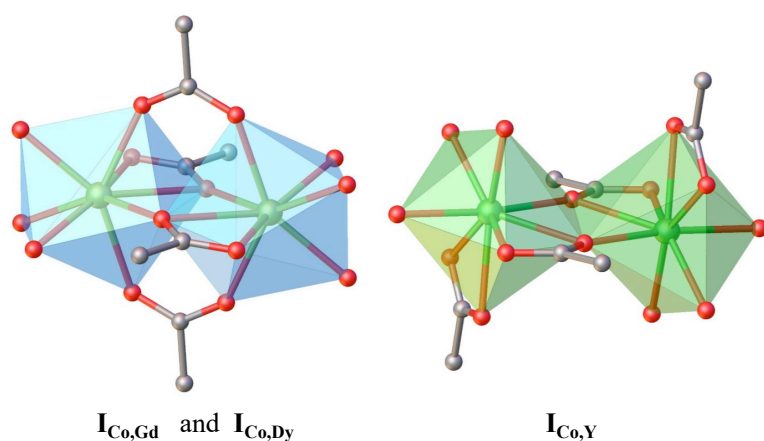


Figure 4. Coordination polyhedra of the $\{\text{Ln}_2\}$ cores in 2p-3d-4f clusters.

It turns out that the apparent similarity of the clusters masks significant differences both for the coordination numbers of the transition metal ions and the geometry of the central lanthanide cores. $\mathbf{I}_{\text{Co,Gd}}$ and $\mathbf{I}_{\text{Co,Dy}}$ ¹⁵ adopt one type of geometry while $\mathbf{I}_{\text{Co,Y}}$ adopt another one. Accordingly, the evolution is not solely driven by the decrease of the ionic radius along the lanthanide series but simultaneously influenced by the nature of the transition metal and that

of the lanthanide. The similarity between $\mathbf{I}_{\text{Co,Gd}}$ and $\mathbf{I}_{\text{Co,Dy}}$ can be pushed further since they crystallize in the same space group and exhibit the same π -stacking of the neutral clusters. Though crystallizing in different space groups, $\mathbf{I}_{\text{Co,Y}}$ exhibit rather similar packing as well with stacking of verdazyl ligands essentially as π -dimers (Figure SI-9).

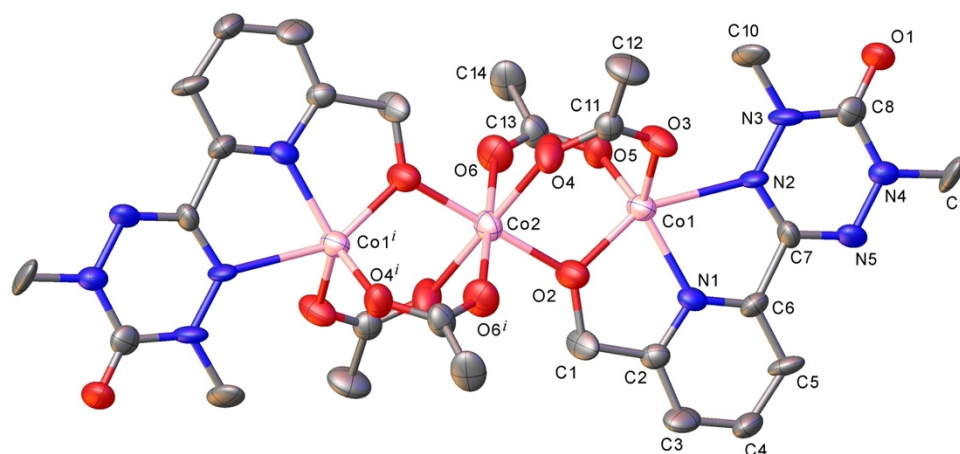


Figure 5. X-ray molecular structure of compound \mathbf{II}_{Co} with atom labeling and thermal ellipsoids at 30% probability. Non-relevant H-atoms are not shown for clarity. Symmetry code: $^i1 - x, 1 - y, 1 - z$.

\mathbf{II}_{Co} crystallizes in the $C2/c$ space group (Table 1). Crystals are composed of neutral molecules of general formula $[(\text{vdpyCH}_2\text{O})_2\text{M}_3(\text{acO})_4]$ (Figure 5). The central cobalt atom Co2 seating on the inversion center, the three-cobalt cluster is centrosymmetric. The outer verdazyl ligands metrics and coordination are similar to the ones observed in the 2p-3d-4f clusters. As in $\mathbf{I}_{\text{Co,Y}}$, the coordination sphere of the Co1 is completed by two oxygen atoms from two $\kappa^2\text{O,O}'(\eta^1:\eta^1:\mu_2)$ bridging acetate, leading to triangular bipyramidal environment for Co1. O5, O3 and N1 atoms, coming from two acetates and the pyridine ring of oxoverdazyl ligand respectively, form the triangular base of the bipyramid (Co1--O3 = 1.975(9), Co1--O5 = 1.956(10), Co1--N1 = 2.055(10) Å). The deviation of Co1 atom from this basal plane is 0.279 Å. The apical positions of the bipyramid are occupied by the bridging oxygen of the deprotonated alkoxo group (Co1--O2 = 1.971 (9) Å) and the nitrogen atom from the verdazyl ring. The long Co1-N2 distance (2.376 (10) Å) once again underlines the modest coordination ability of the verdazyl ring. The central cobalt atom (Co2) has an axially compressed octahedral environment (Co2--O2=1.971(9); Co2--O4 = 2.112(8); Co2--O6 = 2.165(11) Å) with four oxygen from the acetates and two from the alkoxo groups of the radical ligand. According the bond distance analysis,⁴²⁻⁴⁴ the three cobalt atoms exhibit a +II oxidation state and the charge balance is compensated by two deprotonated verdazyl and four deprotonated acetate ligands. The intermolecular interaction between the neutral clusters is dominated by π -stacking between verdazyl ligands favored by their planar configuration (Figures SI-10). In \mathbf{II}_{Co} , the verdazyl ligand form an alternating 1D π - π chains (Figures SI-11). Such π - π interactions are well known in dimethyl-substituted verdazyl in purely organic and coordination compounds. They are known to strongly influence the magnetic properties in the solid state.⁴⁵⁻⁴⁸ Based on X-ray powder diffraction analysis, \mathbf{II}_{Zn} appears to be isostructural with \mathbf{II}_{Co} (Figures SI-12).

Crystals of \mathbf{III}_{Zn} are composed of neutral molecules of general formula $[(\text{vdpyCH}_2\text{OH})\text{Zn}(\text{acO})_2]$ (Figure 6). As for the $\mathbf{I}_{\text{MT,Ln}}$ and \mathbf{II}_{MT} series, the ligand is in its radical form and behave as a tridentate ligand towards Zn(II) but, in contrast to what has been described so far, the alcoholic moiety of the ligand remains protonated. The coordination sphere of the metal ion is completed by two monodentate acetate leading to an overall pentacoordinated triangular bipyramidal environment where the apical positions are occupied by the nitrogen atom of the verdazyl ring and the oxygen atom of the alcoholic

function. Interestingly, this complex really appears as the initial building block in a *in situ* complex-as-ligand approach to yield, upon deprotonation of the alcoholic function, to the formation of the compounds of the $\mathbf{I}_{MT,Ln}$ and \mathbf{II}_{MT} series. The packing of these neutral molecules is governed by π - π interaction between verdazyl-pyridine rings and an intermolecular hydrogen bond implying the hydrogen atom of the alcoholic function. (Figures SI-13,14)

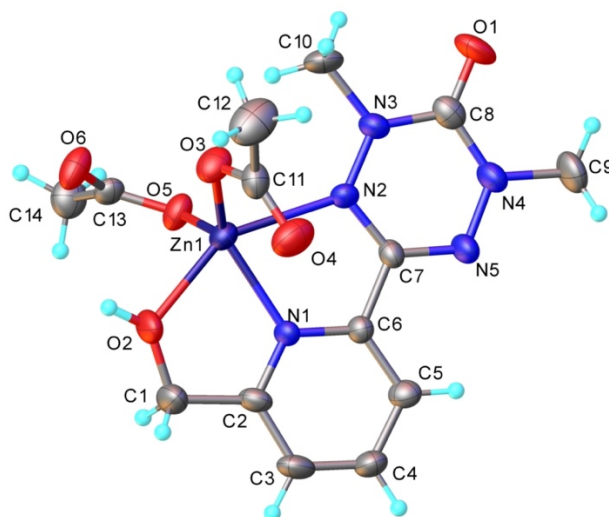


Figure 6. X-ray molecular structure of \mathbf{III}_{Zn} with atom labelling scheme and thermal ellipsoids at 40% level.

This detailed structure analysis is an indication that the chemical substitution approach may have some limitations since the evolution of structural features along the $\mathbf{I}_{MT,Ln}$ series may have a strong influence on magnetic characteristics of the compounds such as magnetic anisotropy and exchange interaction.

Magnetic properties

Static magnetic properties of compounds $\mathbf{I}_{Co,Ln}$ and \mathbf{II}_{TM} were investigated by *dc* magnetometry. The samples were measured as microcrystalline powders between 2 and 300 K under an applied *dc* field of 1000 Oe. Let us start with the simplest compound, which is the one with only one type of spin bearer, \mathbf{II}_{Zn} . The $\chi_M T$ product of \mathbf{II}_{Zn} , χ_M being the molar susceptibility, is worth $0.83 \text{ cm}^3\text{K/mol}$ at room temperature. This is slightly higher than the value expected for the sum of two non-interacting radicals ($0.75 \text{ cm}^3\text{K/mol}$ for $g = 2.0$). The thermal variation of the magnetic susceptibility is shown in Figure 7. Upon cooling, the magnetic susceptibility goes through a rounded maximum before decreasing to a finite value at very low temperature. This behavior is typical of antiferromagnetically (AF) coupled 1D compound. With diamagnetic Zn(II) metal ion, exchange interaction should mainly originate from π - π interactions between the verdazyl radicals. Given that \mathbf{II}_{Zn} and \mathbf{II}_{Co} are isostructural (Figures SI-12), the stacking in \mathbf{II}_{Zn} is considered as alternating. Accordingly, a Heisenberg model for alternating AF chain of spin $S = 1/2$ is used to model the magnetic susceptibility according to the following Hamiltonian:^{49,50}

$$H = -2J \sum_{i=1}^{n/2} [\hat{S}_{2i} \hat{S}_{2i-1} + \alpha \hat{S}_{2i} \hat{S}_{2i+1}]$$

J being the main interaction between nearest neighbors and αJ , the second interaction found along the chain. Fixing $g = 2$, the best fit of the experimental data yields $J = -8.2(1) \text{ cm}^{-1}$ and $\alpha = 0.93(3)$. The determination of this radical-radical intermolecular interaction is very useful to limit the number of free parameters when looking at more complicated compounds exhibiting the same type of stacking.

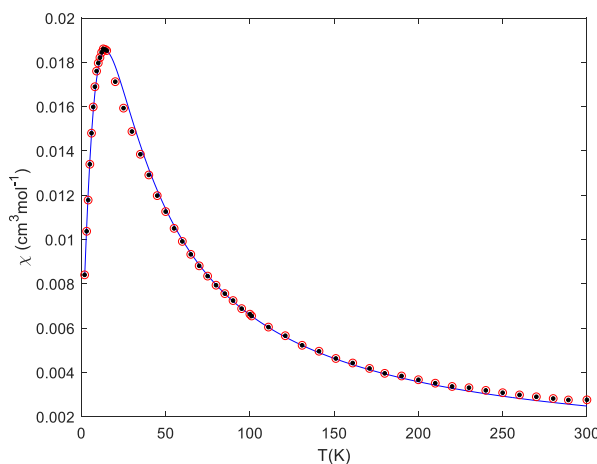


Figure 7. Thermal variations of the magnetic susceptibility for \mathbf{II}_{Zn} . The solid line is the best fit using a Heisenberg alternating AF chain model with $J = -8.2(1) \text{ cm}^{-1}$, $\alpha = 0.93(3)$ and $g = 2(\text{fix})$.

Let us now consider the $\mathbf{I}_{Co,Y}$ case where a noticeable transition metal-radical exchange interaction is present.^{16,51} The $\chi_M T$ value (Figure 8(a)) at high temperature ($5.41 \text{ cm}^3 \text{K} \cdot \text{mol}^{-1}$) is noticeably higher than the sum for four isolated spin bearers with $g = 2.0$ ($4.50 \text{ cm}^3 \text{K} / \text{mol}$ for two $S = 3/2$ and two $S = 1/2$) owing to the orbital contribution to g for the strongly anisotropic Co(II) ions.^{52,53–56} The asymptotic value of the $\chi_M T$ leads to a g_{Co} value of 2.23. When decreasing the temperature, the $\chi_M T$ products gradually decreases with an increasing rate to reach a value of $0.664 \text{ cm}^3 \text{K} \cdot \text{mol}^{-1}$ at 1.92 K. The reduced magnetization curves measured between 2 and 5 K (insert in Figure 9(a)) are far from saturation at 5 T and do not superimpose, revealing a highly anisotropic behaviour of the clusters. To interpret these data, the magnetic entity to be considered does not match with the structural clusters: the diamagnetic $\{Y_2(\text{acO})_4\}$ core indeed cut off the exchange interaction pathways whereas, as shown in \mathbf{II}_{Zn} , the π stacking of the outer verdazyl radicals opens magnetic connections. The system must therefore be modeled as Co-*vd*...*vd*-Co magnetic units involving two isotropic verdazyl radicals ($S=1/2$) and two pentacoordinated anisotropic cobalt(II) ($S=3/2$) centers (Figures 8(b) and SI-9(b)). To unravel anisotropy effects and exchange interactions, it is necessary to consider simultaneously the magnetic susceptibility and the magnetization of $\mathbf{I}_{Co,Y}$ considering multiple contributions, sorted by decreasing expected absolute values:

- i) the orbital contributions of the anisotropic trigonal bipyramidal-coordinated cobalt(II) ions modeled through the ZFS D_{Co} parameter whose value can range from -10 cm^{-1} ^{57,58,59} to $+70 \text{ cm}^{-1}$ ⁶⁰
- ii) ferromagnetic interaction between the radicals and the Co(II) ions with a $J_{Co-*vd*}$ value ranging between $+20$ and $+35 \text{ cm}^{-1}$;^{16,51}
- iii) antiferromagnetic radical-radical interaction with an interaction parameter $J_{*vd-vd*}$ between $-7 \div -8 \text{ cm}^{-1}$ as observed in \mathbf{II}_{Zn} ;

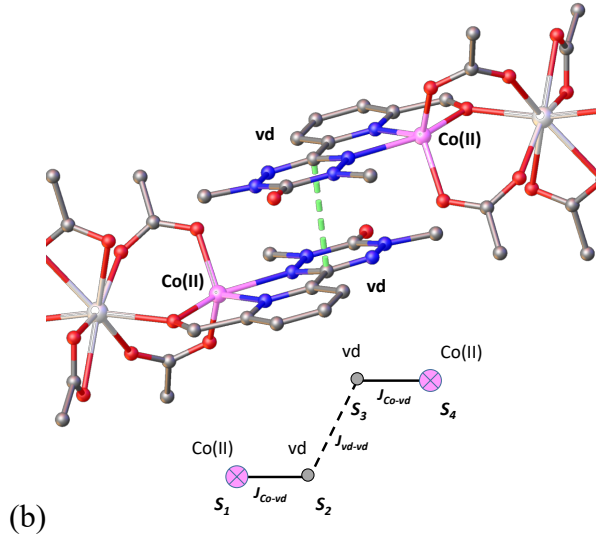
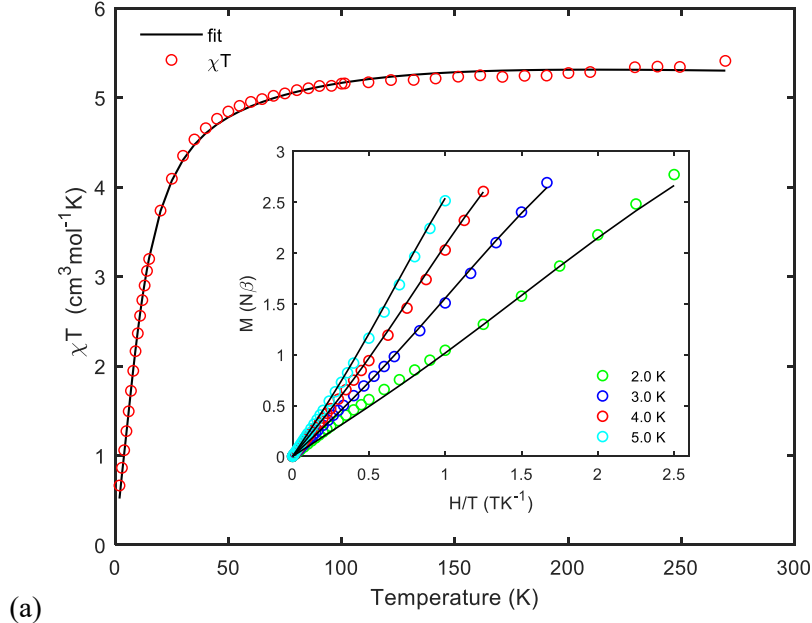


Figure 8. Temperature dependence of magnetic susceptibility and magnetization curves (insert) for ICo_xY ; the black lines correspond to the best fit according the first model described in the text (a) Isolated magnetic units present in ICo_xY (b)

The simultaneous fitting of the whole set of curves (susceptibility and magnetization) was thus undertaken using the following Hamiltonian:

$$\hat{H} = -2J_{\text{Co-vd}}(\vec{S}_1\vec{S}_2 + \vec{S}_3\vec{S}_4) - 2J_{\text{vd-vd}}\vec{S}_2\vec{S}_3 + D_{\text{Co}} \sum_{i=1,4} (\vec{S}_{z_i}^2 - S_i(S_i + 1)/3) + E_{\text{Co}} \sum_{i=1,4} (\vec{S}_{x_i}^2 - \vec{S}_{y_i}^2) + \mu_B \sum_{i=1}^4 g_i \vec{S}_i H$$

with $S_1 = S_4 = 3/2$ (Co(II) centers), $S_2 = S_3 = 1/2$ (verdazyl radicals), $J_{\text{Co-vd}}$ and $J_{\text{vd-vd}}$, the Co-vd and vd...vd exchange interaction parameters and D_{Co} and E_{Co} , the ZFS parameters^{61,57,58,60,62} for the pentacoordinated cobalt(II) centers and the Zeeman interaction. From the literature and the results obtained above, the initial values for the fitting parameters were taken as $g_{\text{Co}} = 2.2$, $D_{\text{Co}} = 50.0 \text{ cm}^{-1}$, $E_{\text{Co}} = 10.0 \text{ cm}^{-1}$, $J_{\text{Co-vd}} = +25.0 \text{ cm}^{-1}$,^{16,51} $J_{\text{vd-vd}} = -7.0 \text{ cm}^{-1}$, $g_{\text{vd}} = 2.0$ (fixed). The outcome of the simultaneous fitting procedure is $g_{\text{Co}} = 2.13(4)$, $D_{\text{Co}} = 100(2) \text{ cm}^{-1}$, $E_{\text{Co}} =$

19.9(5) cm⁻¹, $J_{Co-vd} = +26.5(4)$ cm⁻¹ and $J_{vd-vd} = -7.95(4)$ cm⁻¹ (Figure 8(a)). The simultaneous fitting procedure combined with the fact that the final parameters compare well with those found in situations where the structural features are pretty similar to the one observed in **I**_{Co,Y} increase the confidence in the meaningfulness of the set of parameters extracted from the fit. This is of utmost importance for such situations where several competing contributions influence the magnetic properties of the system.

Given the value of the D_{Co} parameter of 100 cm⁻¹, obtained for the former magnetic susceptibility analysis, much higher than the other parameters ruling the system, it is reasonable, and interesting for comparison, to treat the cobalt(II) centers in the effective spin model. This approach has been successfully applied to model the magnetic interaction between strongly anisotropic Co(II) ion with different organic radicals.^{63,64,65,66} According to ligand field theory, the trigonal bipyramidal distribution of the donating atoms around the Co(II) center will split the 3d orbitals in three groups of orbitals (Figure 9).^{67,68,69,70,71}

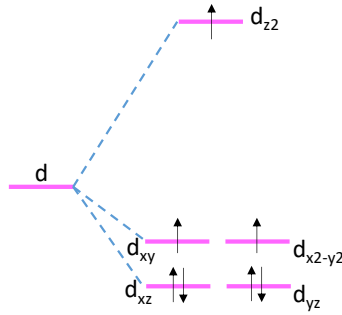


Figure 9. Energy of 3d orbital of Co(II) in the trigonal bipyramidal crystal field.

The trigonal bipyramidal geometrical configuration of crystal field add significant contribution to axial ZFS parameter (D_{Co}) of Co(II) and stabilize the $\pm 1/2$ components of ground state.^{61,72} Taking into account the values of the D_{Co} ZFS parameter, at low temperature ($T < 30$ K) only the ground Kramers doublet is populated. In these conditions, the pseudo-spin $1/2$ Hamiltonian^{73,74,75,76-78,79,80} can be applied in order to describe the magnetic interaction between the verdazyl radical and Co(II) paramagnetic centers:

$$\widehat{H}_{ex} = -2J_{Co-vd}^{eff} (\vec{S}_{1eff}\vec{S}_2 + \vec{S}_3\vec{S}_{4eff}) - 2J_{vd-vd}\vec{S}_2\vec{S}_3$$

were $S_{1eff} = S_{4eff} = 1/2$ is the effective spin of cobalt, J_{Co-vd}^{eff} is the rank one tensor of anisotropic Co(II)-Vd exchange interaction and J_{vd-vd} is the isotropic exchange interaction between verdazyl ligands as in the previous model. The first-order Zeeman terms are also taken into account with isotropic fixed g-factor for verdazyl radical (2.0) and anisotropic ones for cobalt(II).

In order to decrease the number of variable parameters, we limit ourselves to axial symmetry^{76,81} for the g_{Co} and J_{Co-vd} tensors, e.g. $J_{Co-vd}^{xx} = J_{Co-vd}^{yy} = J_{Co-vd}^{\perp}$; $J_{Co-vd}^{zz} = J_{Co-vd}^{\parallel}$; $g_{Co}^{xx} = g_{Co}^{yy} = g_{Co}^{\perp}$; $g_{Co}^{zz} = g_{Co}^{\parallel}$. The best fit using the effective spin model is presented in Figure SI-15. It corresponds to the following parameters: $J_{Co-vd}^{\perp} = -0.0 \pm 2$ cm⁻¹; $J_{Co-vd}^{\parallel} = +27.8 \pm 0.5$ cm⁻¹; $J_{vd-vd} = -18.8 \pm 0.3$ cm⁻¹; $g_{Co}^{\perp} = 5.0 \pm 0.1$; $g_{Co}^{\parallel} = 4.1 \pm 0.1$. The obtained g_{Co} factors of Co(II) values are close to expected effective g-factor for high spin

Co(II) (3.8-4.3)⁶⁵ whereas the J tensor definitely corresponds to a well-defined Ising-type ferromagnetic interaction.

To conclude, the two approaches are sensitive to the existence of the ferromagnetic interaction between the Co(II) ion and the verdazyl radical. The differences in the absolute values of the extracted parameters indicate that the direct comparison of parameters obtained using different models is much questionable. Accordingly, such comparisons must be undertaken with utmost care to remain meaningful.

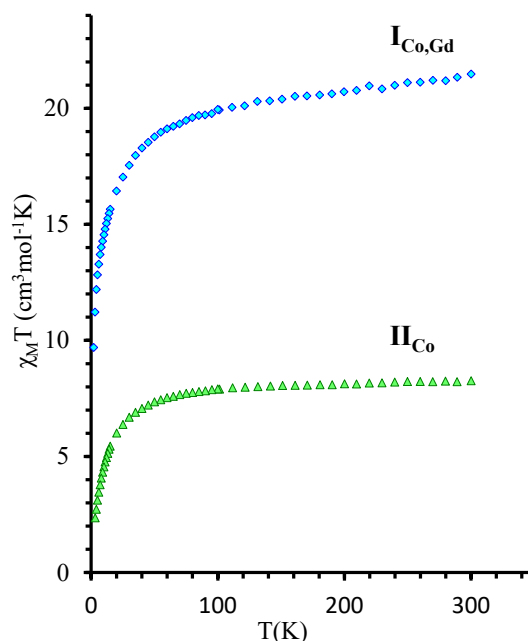


Figure 10. Temperature dependence of the magnetic susceptibility for $\mathbf{I}_{\text{Co,Gd}}$ and \mathbf{II}_{Co} .

The thermal variations of the magnetic susceptibility of $\mathbf{I}_{\text{Co,Gd}}$ and \mathbf{II}_{Co} (Figure 10) have essentially the same shape compared to that of $\mathbf{I}_{\text{Co,Y}}$, the main change being the value of the $\chi_M T$ product at room temperature. For $\mathbf{I}_{\text{Co,Gd}}$, the $\chi_M T$ value at room temperature is 21.48 $\text{cm}^3\text{K/mol}$ which is higher than the sum for the isolated spin centers forming the cluster, e.g. 20.26 $\text{cm}^3\text{K/mol}$ for two Gd^{III} ions ($S=7/2$, $g=2.0$, 15.76 $\text{cm}^3\text{K/mol}$), two Co(II) ions ($S=3/2$, $g=2.0$, 3.75 $\text{cm}^3\text{K/mol}$) and two oxoverdazyl radicals ($S=1/2$, $g=2.0$, 0.75 $\text{cm}^3\text{K/mol}$) (Figure 10). For \mathbf{II}_{Co} , the $\chi_M T$ value at room temperature is 8.26 $\text{cm}^3\text{K/mol}$ which is higher than the sum for the isolated spin centers forming the cluster, e.g. 6.375 $\text{cm}^3\text{K/mol}$ for three Co(II) ions ($S=3/2$, $g=2.0$, 5.625 $\text{cm}^3\text{K/mol}$) and two oxoverdazyl radicals ($S=1/2$, $g=2.0$, 0.75 $\text{cm}^3\text{K/mol}$) (Figure 9). Once again, the difference can be ascribed to the orbital contribution to g_{Co} . For $\mathbf{I}_{\text{Co,Gd}}$ a value of $g_{\text{Co}}=2.23$ for the Co(II) ions allows to retrieve the experimental value. For \mathbf{II}_{Co} , g_{Co} must reach an average value of 2.32 to retrieve the experimental value. This higher value of the average gyromagnetic factor g_{Co} compared to $\mathbf{I}_{\text{Co,Y}}$ is ascribed to the octahedral cobalt(II) ion at the center of the cluster. The thermal variations of $\chi_M T$ for $\mathbf{I}_{\text{Co,Gd}}$ is comparable to that of $\mathbf{I}_{\text{Co,Y}}$ with a more rounded decrease at low temperature to reach 9.70 $\text{cm}^3\text{K/mol}$ at 2.0 K. These changes are related to the presence of a third (anisotropic) spin bearer in the considered clusters.

By creating Co-Gd and Gd-Gd (for $\mathbf{I}_{\text{Co,Gd}}$) and Co-Co (for \mathbf{II}_{Co}) exchange interactions, this third paramagnetic partner(s) reconnect the isolated Co-vd...vd-Co discrete magnetic units present in $\mathbf{I}_{\text{Co,Y}}$, totally changing the magnetic modelling. Moreover, the central octahedral cobalt(II) center should be treated using a spin-orbital approach rather than the phenomenological ZFS or effective spin approaches. Altogether, this complexification prevents any further analysis of the *dc* magnetic behaviour of these species.

Our previous study¹⁵ revealed that $\mathbf{I}_{\text{Co,Dy}}$ exhibits a slow relaxation of the magnetization with a U_{eff} around 15K, the reversal being favored essentially by quantum tunnel of magnetization (QTM). The dynamic properties of $\mathbf{I}_{\text{Co,Gd}}$ and $\mathbf{I}_{\text{Co,Y}}$ were studied by measuring the temperature and field dependence of the *ac* (alternative current) magnetic susceptibility in the very same conditions as for $\mathbf{I}_{\text{Co,Dy}}$.

For both compounds, where the two cobalt(II) ions are the only anisotropic magnetic centers, no signal was observed in the out-of-phase component (χ''_{ac}) of the *ac* magnetic susceptibility measured in zero *dc* field. Applying *dc* fields below 2000 Oe did not change the situation. Does it rule out the cobalt centers as the source of the slow magnetic relaxation in $\mathbf{I}_{\text{Co,Dy}}$? From the structural, analysis, it appears that the environment of the cobalt(II) ion is slightly different in $\mathbf{I}_{\text{Co,Dy}}$ and $\mathbf{I}_{\text{Co,Y}}$ going from six-coordinated to five-coordinated. The sensitivity of magnetic anisotropy to the details of the coordination environment could explain the disappearance of the slow relaxation behavior when going from $\mathbf{I}_{\text{Co,Dy}}$ and $\mathbf{I}_{\text{Co,Y}}$. Fortunately, in $\mathbf{I}_{\text{Co,Gd}}$, the coordination environment of the transition metal ion is much comparable to the one observed in $\mathbf{I}_{\text{Co,Dy}}$ and Gd(III) does not bring any magnetic anisotropy to the system. It thus appears that cobalt(II) is not the main source of slow relaxation of the magnetization in this family of 2p-3d-4f clusters.

Conclusion

We report on the synthesis of two series of clusters $\mathbf{I}_{\text{Co,Ln}}$ (Ln=Y(III), Gd(III)) and \mathbf{II}_{MT} (MT=Zn(II), Co(II)) obtained by self-assembly combining 1,5-dimethyl-3-(3'-(hydroxymethyl)-2'-pyridine)-6-oxotetrazane ($\text{H}_3\text{vdpyCH}_2\text{OH}$) or its oxidized verdazyl form with transition metal and/or lanthanide acetates. The isolation of \mathbf{III}_{Zn} , a mononuclear complex of formula $[(\text{vdpyCH}_2\text{OH})\text{Zn}(\text{acO})_2]$, as a secondary product allows to propose this initial complex as the key building block towards the 2p-3d-4f clusters $\mathbf{I}_{\text{MT,Ln}}$ and the 2p-3d clusters \mathbf{II}_{MT} through a *in situ* complex-as-ligand approach.

Detailed single-crystal diffraction studies confirm¹⁵ that $\mathbf{I}_{\text{MT,Ln}}$ series is composed of centrosymmetric clusters with verdazyl radicals at the periphery, coordinated to the transition metal ion in a tridentate mode and to the lanthanide $\{\text{Ln}_2(\text{acO})_4\}$ central core by its alkoxo moiety, the metal ions being further bridged by acetate ions to yield $[(\text{vdpyCH}_2\text{O})_2\text{M}_2\text{Ln}_2(\text{acO})_8]$ clusters. It appears that the coordination environment of both the transition and lanthanide metal ions are influenced by chemical substitution: in $\mathbf{I}_{\text{Co,Gd}}$, the transition metal ions is in irregular octahedral environment and the $\{\text{Gd}_2(\text{acO})_4\}$ central core adopts a paddlewheel motif whereas in $\mathbf{I}_{\text{Co,Y}}$ the transition metal is pentacoordinated and the central core contains only two acetate bridges. The evolution of the coordination sphere for the transition and lanthanide ions are synergetic with a combined influence of the nature of the transition metal ion and of the lanthanide. The compounds within the \mathbf{II}_{MT} series are composed of centrosymmetric clusters with verdazyl radicals at the periphery, coordinated in a tridentate mode to a first transition metal ion in a triangular bipyramidal pentacoordinated environment and to a second transition metal ion in an octahedral environment by its alkoxo moiety, the metal ions being further bridged by acetate ions to yield $[(\text{vdpyCH}_2\text{O})_2\text{M}_3(\text{acO})_4]$ clusters.

The measurements and analysis of the *dc* magnetic properties revealed that, within the two series, the π -stacked outer verdazyl radicals are antiferromagnetically (AF) coupled with exchange interaction parameters being in the $-7.5 \div -8.5 \text{ cm}^{-1}$ range. In $\mathbf{I}_{\text{Co,Y}}$, the demanding fitting procedure of both the

magnetic susceptibility and the reduced magnetization $M=f(H/T)$ allowed to extract with a good confidence the relevant magnetic parameter of the system, e.g. $g_{Co} = 2.13(4)$, $D = 100(2) \text{ cm}^{-1}$ and $E = 19.9(5) \text{ cm}^{-1}$, $J_{Co-vd} = +26.5(4) \text{ cm}^{-1}$ and $J_{vd-vd} = -7.95(4) \text{ cm}^{-1}$. Such a procedure could not be extended to systems with three different spin bearers forming magnetic units and ruled by a welfare of parameters. Finally, *ac* magnetic susceptibility studies revealed that, in contrast with the parent compound $\mathbf{I}_{Co,Dy}$, neither $\mathbf{I}_{Co,Gd}$ nor $\mathbf{I}_{Co,Y}$ show any slow relaxation of the magnetization. Though slight structural evolutions occur during the chemical substitution at both metal centers, it can be concluded that the cobalt(II) centers do not play the central role in the slow relaxation of the magnetization in this series of 2p-3d-4f clusters.

To conclude, this study shows that chemical substitution is a powerful tool for understanding the synthesis, structural and magnetic properties of complex heterometallic magnetic clusters but it underlines that this approach has inherent limitations related to subtle structural modifications around the metal ions that can have noticeable influence onto their magnetic properties. Despite these limitations, the examination of clusters associating Dy(III) with diamagnetic or isotropic transition metal ions is mandatory to have a complete view, in particular, about the origin of the slow relaxation of the magnetization, of these 2p-3d-4f clusters.

Experimental Section

Materials. All chemicals were of reagent grade quality. They were purchased from commercial sources and used as received. Bis(1-methylhydrazide)carbonic acid was prepared by a previously reported method.¹⁵

Synthesis of 1,5-dimethyl-3-(6'-(hydroxymethyl)-2'-pyridine)-6-oxotetrazane ($\mathbf{H}_3\text{vdpyCH}_2\text{OH}$)

3.28 g (23.94 mmol) 6-(hydroxymethyl)-2-pyridinecarbaldehyde was dissolved in 100 mL methanol by refluxing. The resulting solution was added dropwise into a 100 mL methanol solution containing 2.54 g (23.96 mmol) of *bis*(1-methylhydrazide)carbonic acid. The reaction mixture was refluxed overnight. After refluxing, the reaction mixture was cooled, evaporated and recrystallized from dichloromethane or methanol. Yield = 87.4. Anal. Calcd for $\text{C}_{10}\text{H}_{15}\text{N}_5\text{O}_2$ (MW 237 g mol⁻¹), %: C, 50.62; H, 6.37; N, 29.52. Found, %: C, 51.14; H, 6.26; N, 29.32. See the ¹H and ¹³C spectra in Figure SI-5,6 and FTIR spectra in Figure SI-4.

Synthesis of Verdazyl Radical vdpyCH_2OH , 6-(6-(hydroxymethyl)pyridine-2-yl)-2,4-dimethyl-1,4-dihydro-1,2,4,5-tetrazin-3(2H)-one

0.24 g (1.0 mmol) of 2-tetrazane-6-(hydroxymethyl)pyridine was dissolved in 20mL distilled dichloromethane. To this solution was added a solution of 0.16 g (1.48 mmol) 1,4-benzoquinone in 10 mL of the same solvent. The reaction mixture was kept on stirring while heating at 40°C and gradually it becomes brown. Distilled dichloromethane was regularly added to maintain the volume of the solution. After two hours, a brown precipitate was formed. The reaction mixture was then filtered and purified by column chromatography (with 5% methanol in dichloromethane). Yield = 43.5%. See FTIR spectra in Figure SI-1

Synthesis of \mathbf{II}_{Co} , $[(\text{vdpyCH}_2\text{O})_2\text{Co}_3(\text{acO})_4]$

0.12 g (0.5 mmol) of $\mathbf{H}_3\text{vdpyCH}_2\text{OH}$ was dissolved in 15 mL acetonitrile. To this solution was added 0.12 g (0.48 mmol) cobalt(II) acetate tetrahydrate. The reaction mixture was put on stirring for around 20 minutes until a clear mixture was obtained. The mixture was then filtered. Filtrate was left at room temperature for 4-5 hours to have crystals of the desired

compound suitable for single X-ray diffraction, which was filtrated and washed with cool acetonitrile. Yield = 48.7%. Anal. Calcd for $C_{28}H_{34}Co_3N_{10}O_{12}$ (MW 879.44 g mol⁻¹), %: C, 38.24; H, 3.90; N, 15.93; Found, %: C, 38.60; H, 3.86; N, 15.86. (See the FTIR spectra in Figure SI-3).

Synthesis of **II**_{Zn}, [(vdpyCH₂O)₂Zn₃(acO)₄]

0.06 g (0.25 mmol) of **vdpyCH₂OH** was dissolved in 10 mL acetonitrile in which 0.083 g (0.37 mmol) of solid zinc(II) acetate dehydrate was added. After stirring, a clear red solution was obtained. The reaction mixture was stirred around 1 hour and a brown compound crystalize. At room temperature, this mixture was filtered and filtrate was dried on air for few hours to have desired compound. Yield = 43.5%. Anal. Calcd for $C_{28}H_{34}Zn_3N_{10}O_{12}$ (MW 898.78 g mol⁻¹), %: C, 37.42; H, 3.81; N, 15.58; Found, %: C, 37.68; H, 3.96; N, 15.46. See the FTIR spectra in SI).

Synthesis of **I**_{Co,Ln} (Ln = Gd^{III}, Y^{III}) = [(vdpyCH₂O)₂Co₂Ln₂(acO)₈]

0.12 g (0.5 mmol) tetrazane was dissolved in 15 mL acetonitrile. For **I**_{Co,Gd}, to this solution, 0.10 g (0.246 mmol) of gadolinium(III) acetate tetrahydrate was added (for **I**_{Co,Y}, 0.085 g (0.25 mmol) of yttrium(III) acetate tetrahydrate was added). The reaction mixture was stirred for 30 minutes until a clear mixture was obtained. Then, mixture was filtered and the filtrate was left at room temperature for a few hours to yield single crystals of the desired compound. **I**_{Co,Gd} Yield = 55.4% Anal. Calcd for $C_{36}H_{46}Co_2Gd_2N_{10}O_{20}$ (MW 1371.18 g mol⁻¹), %: C, 31.53; H, 3.38; N, 10.22; Found, %: C, 31.83; H, 3.48; N, 10.30. **I**_{Co,Y} Yield = 66.2%. Anal. Calcd for $C_{36}H_{46}Co_2N_{10}O_{20}Y_2 \cdot 2(C_2H_3N)$ (MW 1316.60 g mol⁻¹), %: C, 36.49; H, 3.98; N, 12.77; Found, %: C, 36.09; H, 4.06; N, 12.60. See the FTIR spectra in Figure SI-2.

X-ray crystallography. X-ray diffraction measurements were carried out with an Oxford-Diffraction XCALIBUR E CCD diffractometer equipped with graphite-monochromated Mo-K α radiation for **H₄L^{DCM}**, **II**_{Co}, and SuperNova diffractometer using hi-flux micro-focus Nova Cu-K α radiation for **I**_{Co,Y}, **I**_{Co,Gd} and **III**_{Zn}. Single crystals were positioned at 40 mm from the detector and 292, 238, 376, 887, 277 and 569 frames were measured each for 80, 240, 1, 2, 75 and 70 s over 1° scan width, respectively. X-ray data collection for **H₄L^{MeOH}** was performed on a Bruker P4 diffractometer using Ag-K α radiation. The unit cell determination and data integration were carried out using the CrysAlis package of Oxford Diffraction.⁵³ The structures were solved by direct methods using Olex2⁸² and refined by full-matrix least-squares on F^2 with SHELXL-2015⁸³ using an anisotropic model for non-hydrogen atoms. All H atoms were introduced in idealised positions ($d_{CH} = 0.96 \text{ \AA}$) using the riding model. The positional parameters for hydroxyl groups and water molecules were determined from Fourier maps and verified by H-bonds parameters. The molecular plots were obtained using the Olex2 program. The crystallographic data and refinement details are quoted in Tables 1, while bond lengths and angles are summarised in Table S1. CCDC - 1965686 (**H₄L^{DCM}**), CCDC - 1965687 (**II**_{Co}), CCDC - 1965688 (**I**_{Co,Y}), CCDC 1968217 (**I**_{Co,Gd}), CCDC1965690 (**III**_{Zn}) and CCDC 1965693 (**H₄L^{MeOH}**) contain the supplementary crystallographic data for this contribution. These data can be obtained free of charge via www.ccdc.cam.ac.uk/conts/retrieving.html (or from the Cambridge Crystallographic Data Centre, 12 Union Road, Cambridge CB2 1EZ, UK; fax: (+44) 1223-336-033; or deposit@ccdc.ca.ac.uk)

Magnetometry *dc* magnetic susceptibility data (2-300K) were collected on powdered samples using a SQUID magnetometer (Quantum Design MPMS-XL), applying a magnetic field of 0.1 T. All data were corrected for the contribution of the sample holder and the diamagnetism of the samples estimated from Pascal's constants.^{84,52} The field dependence of the magnetization

(up to 5 T) was measured between 2.0 and 5.0 K. For analyzing *dc* susceptibility data, we used the PHI software.⁸⁵ *ac* magnetic susceptibility was measured at 2.0K with an oscillating field magnitude of $H_{ac}=3.0$ Oe and frequency ranging between 1 and 1488 Hz in presence of a *dc* field.

The **FTIR** spectra were recorded with 16 scans per spectrum at a resolution of 4 cm^{-1} using the Nicolet Fourier Transform Infra-Red (FTIR) spectrophotometer iS 50 IR.

Table 1. Crystal data and details of data collection.

Compound	H ₃ vdCH ₂ OH (H ₄ L ^{DCM})	H ₃ vdCH ₂ OH (H ₄ L ^{MeOH})	I _{Co,Y}	I _{Co,Gd}	II _{Co}	III _{Zn}
empirical formula	C ₁₀ H ₁₅ N ₅ O ₂	C ₁₀ H ₁₅ N ₅ O ₂	C ₂₀ H ₂₆ CoN ₆ O ₁₀ Y	C ₁₈ H ₂₃ CoGdN ₅ O ₁₀	C ₂₈ H ₃₄ Co ₃ N ₁₀ O ₁₂	C ₁₆ H ₂₁ N ₆ O ₆ Zn
<i>F</i> _w	237.27	237.27	658.31	685.59	879.44	458.76
<i>T</i> [K]	160	293(2)	293(2)	293	293(2)	293(2)
space group	<i>P</i> 2 ₁ / <i>c</i>	P-1	<i>P</i> 2 ₁ / <i>c</i>	P-1	<i>C</i> 2/ <i>c</i>	<i>C</i> <i>c</i>
<i>a</i> [Å]	20.8514(16)	7.9816(16)	10.0428(3)	10.2463(8)	8.112(2)	10.4165(9)
<i>b</i> [Å]	7.9608(5)	8.0785(16)	19.3361(5)	10.7803(9)	23.146(6)	27.0875(16)
<i>c</i> [Å]	14.8743(14)	10.004(2)	14.2059(3)	13.2769(8)	18.990(6)	7.5800(7)
<i>α</i> [°]	90	92.56(3)	90	108.860(7)	90	90
<i>β</i> [°]	110.654(9)	103.03(3)	96.495(2)	93.913(6)	99.28(3)	110.893(10)
<i>γ</i> [°]	90	111.26(3)	90	117.254(8)	90	90
<i>V</i> [Å ³]	2310.3(3)	580.0(2)	2740.92(11)	1192.29(18)	3519.0(17)	1998.1(3)
<i>Z</i>	8	2	4	2	4	4
<i>r</i> _{calcd} [g cm ⁻³]	1.364	1.359	1.595	1.910	1.660	1.525
<i>m</i> [mm ⁻¹]	0.100	0.062	8.113	23.809	1.473	1.275
Crystal size [mm]	0.40 × 0.10 × 0.10	0.15 × 0.10 × 0.05	0.40 × 0.05 × 0.05	0.35 × 0.03 × 0.02	0.08 × 0.03 × 0.01	0.05 × 0.03 × 0.02
2Θ range	4.176 to 50.048	5.8 to 42.84	7.754 to 133.196	9.788 to 133.172	7.042 to 46.508	5.976 to 46.51
Reflections collected	4070	5517	10263	7017	5940	7734
Independent reflections	4070 [<i>R</i> _{int} = 0.0803]	2558 [<i>R</i> _{int} = 0.0961]	4824 [<i>R</i> _{int} = 0.0393]	4139 [<i>R</i> _{int} = 0.0889]	2512 [<i>R</i> _{int} = 0.1578]	2751 [<i>R</i> _{int} = 0.0495]
Data/restraints/parameters	4070/0/314	2558/0/226	4824/0/350	4139/0/322	2512/1/245	2751/2/253
GOF ^[c]	1.048	1.098	1.013	0.937	0.992	1.056
<i>R</i> ₁ ^[d]	0.0638	0.0690	0.0433	0.0555	0.0960	0.0417
<i>wR</i> ₂ ^[b]	0.1413	0.1977	0.10961	0.1086	0.2196	0.0918
Largest diff. peak/hole / e Å ⁻³	0.39/-0.25	0.30/-0.30	0.66/-0.40	0.87/-1.04	0.77/-0.41	0.26/-0.24
Flack parameter	-	-	-	-	-	0.025(12)

^[d]*R*₁ = Σ||*F*_o - |*F*_c||/Σ|*F*_o|. ^[b]*wR*₂ = {Σ[*w*(*F*_o² - *F*_c²)/Σ(*w*(*F*_o²))}]^{1/2}. ^[c]GOF = {Σ[*w*(*F*_o² - *F*_c²)]/(*n* - *p*)}^{1/2}, where *n* is the number of reflections and *p* is the total number of parameters refined.

References

- (1) Sessoli, R.; Gatteschi, D.; Caneschi, A.; Novak, M. A. Magnetic Bistability in a Metal-Ion Cluster. *Nature* **1993**, *365* (6442), 141–143. <https://doi.org/10.1038/365141a0>.
- (2) Vaidya, S.; Shukla, P.; Tripathi, S.; Rivière, E.; Mallah, T.; Rajaraman, G.; Shanmugam, M. Substituted versus Naked Thiourea Ligand Containing Pseudotetrahedral Cobalt(II) Complexes: A Comparative Study on Its Magnetization Relaxation Dynamics Phenomenon. *Inorg. Chem.* **2018**, *57* (6), 3371–3386. <https://doi.org/10.1021/acs.inorgchem.8b00160>.
- (3) Vallejo, J.; Castro, I.; Ruiz-García, R.; Cano, J.; Julve, M.; Lloret, F.; De Munno, G.; Wernsdorfer, W.; Pardo, E. Field-Induced Slow Magnetic Relaxation in a Six-Coordinate Mononuclear Cobalt(II) Complex with a Positive Anisotropy. *J. Am. Chem. Soc.* **2012**, *134*, 15704.
- (4) Gomez-Coca, S.; Urtizberea, A.; Cremades, E.; Alonso, P. J.; Camon, A.; Ruiz, E.; Luis, F. Origin of Slow Magnetic Relaxation in Kramers Ions with Non-Uniaxial Anisotropy. *Nat. Commun.* **2014**, *5*, 4300.
- (5) Zhang, Y.-Z.; Gomez-Coca, S.; Brown, A. J.; Saber, M. R.; Zhang, X.; Dunbar, K. R. Trigonal Antiprismatic Co(II) Single Molecule Magnets with Large Uniaxial Anisotropies: Importance of Raman and Tunneling Mechanisms. *Chem. Sci.* **2016**, *7*, 6519.
- (6) Novikov, V. V.; Pavlov, A. A.; Nelyubina, Y. V.; Boulon, M.-E.; Varzatskii, O. A.; Voloshin, Y. Z.; Winpenny, R. E. P. A Trigonal Prismatic Mononuclear Cobalt(II) Complex Showing Single-Molecule Magnet Behavior. *J. Am. Chem. Soc.* **2015**, *137*, 9792.
- (7) Colacio, E.; Ruiz, J.; Ruiz, E.; Cremades, E.; Krzystek, J.; Carretta, S.; Cano, J.; Guidi, T.; Wernsdorfer, W.; Brechin, E. K. Slow Magnetic Relaxation in a CoII–YIII Single-Ion Magnet with Positive Axial Zero-Field Splitting. *Angew. Chem., Int. Ed.* **2013**, *52*, 9130.
- (8) Ding, Y.-S.; Yu, K.-X.; Reta, D.; Ortu, F.; Winpenny, R. E. P.; Zheng, Y.-Z.; Chilton, N. F. Field- and Temperature-Dependent Quantum Tunneling of the Magnetisation in a Large Barrier Single-Molecule Magnet. *Nat. Commun.* **2018**, *9* (1), 3134. <https://doi.org/10.1038/s41467-018-05587-6>.
- (9) Soc, C. Chem Soc Rev. *Chem. Soc. Rev.* **2015**, *44*, 6655–6669. <https://doi.org/10.1039/C5CS00222B>.
- (10) Liu, J.; Chen, Y. C.; Liu, J. L.; Vieru, V.; Ungur, L.; Jia, J. H.; Chibotaru, L. F.; Lan, Y.; Wernsdorfer, W.; Gao, S.; Chen, X. M.; Tong, M. L. A Stable Pentagonal Bipyramidal Dy(III) Single-Ion Magnet with a Record Magnetization Reversal Barrier over 1000 K. *J. Am. Chem. Soc.* **2016**, *138* (16), 5441–5450. <https://doi.org/10.1021/jacs.6b02638>.
- (11) Goodwin, C. A. P.; Ortu, F.; Reta, D.; Chilton, N. F.; Mills, D. P. Molecular Magnetic Hysteresis at 60 Kelvin in Dysprosocenium. *Nature* **2017**, *548* (7668), 439–442. <https://doi.org/10.1038/nature23447>.
- (12) Sessoli, R.; Powell, A. K. Strategies towards Single Molecule Magnets Based on Lanthanide Ions. *Coord. Chem. Rev.* **2009**, *253* (19–20), 2328–2341. <https://doi.org/10.1016/j.ccr.2008.12.014>.
- (13) Andruh, M.; Costes, J.; Diaz, C.; Gao, S. ID 380 3d - 4f Combined Chemistry : Synthetic Strategies and Magnetic Properties. *Inorg. Chem.* **2009**, *48* (8), 3342–3359. <https://doi.org/10.1021/ic801027q>.
- (14) Andruh, M. Heterotrimetallic Complexes in Molecular Magnetism. *Chem. Commun.* **2018**, *54* (29), 3559–3577. <https://doi.org/10.1039/C8CC00939B>.
- (15) Novitchi, G.; Shova, S.; Lan, Y.; Wernsdorfer, W.; Train, C. Verdazyl Radical, a Building Block for a Six-Spin-Center 2p-3d-4f Single-Molecule Magnet. *Inorg. Chem.* **2016**, *55* (23), 12122–12125. <https://doi.org/10.1021/acs.inorgchem.6b02380>.
- (16) Barclay, T. M.; Hicks, R. G.; Lemaire, M. T.; Thompson, L. K.; Xu, Z. Synthesis and Coordination Chemistry of a Water-Soluble Verdazyl Radical. Structures and Magnetic Properties of M(H₂O)₂(VdCO₂)₂·2H₂O (M = Co, Ni; VdCO₂ = 1,5-Dimethyl-6-Oxo-Verdazyl-3-Carboxylate). *Chem. Commun.* **2002**, No. 16, 1688–1689. <https://doi.org/10.1039/B204851E>.
- (17) Brook, D. J. R.; Fornell, S.; Noll, B.; Yee, G. T.; Koch, T. H. Synthesis and Structure of Di-μ-Bromo-

- Bis[(1,5-Dimethyl-6-Oxo-3-(2-Pyridyl)Verdazyl)Copper(I)]. *J. Chem. Soc. Dalt. Trans.* **2000**, 3 (13), 2019–2022. <https://doi.org/10.1039/a908563g>.
- (18) Norel, L.; Rota, J. B.; Chamoreau, L. M.; Pilet, G.; Robert, V.; Train, C. Spin Transition and Exchange Interaction: Janus Visions of Supramolecular Spin Coupling between Face-to-Face Verdazyl Radicals. *Angew. Chemie - Int. Ed.* **2011**, 50 (31), 7128–7131. <https://doi.org/10.1002/anie.201101190>.
- (19) Norel, L.; Pointillart, F.; Train, C.; Chamoreau, L.-M.; Boubekour, K.; Journaux, Y.; Brieger, A.; Brook, D. J. R. Imidazole-Substituted Oxoverdazyl Radical as a Mediator of Intramolecular and Intermolecular Exchange Interaction. *Inorg. Chem.* **2008**, 47 (7), 2396–2403. <https://doi.org/10.1021/ic701400b>.
- (20) Barr, C. L.; Chase, P. A.; Hicks, R. G.; Lemaire, M. T.; Stevens, C. L. Synthesis and Characterization of Verdazyl Radicals Bearing Pyridine or Pyrimidine Substituents: A New Family of Chelating Spin-Bearing Ligands. *J. Org. Chem.* **1999**, 64 (24), 8893–8897. <https://doi.org/10.1021/jo991198c>.
- (21) Barr, C. L.; Chase, P. A.; Hicks, R. G.; Lemaire, M. T.; Stevens, C. L. Synthesis and Characterization of Verdazyl Radicals Bearing Pyridine or Pyrimidine Substituents: A New Family of Chelating Spin-Bearing Ligands. *J. Org. Chem.* **1999**, 64 (24), 8893–8897. <https://doi.org/10.1021/jo991198c>.
- (22) Hicks, R. G.; Lemaire, M. T.; Öhrström, L.; Richardson, J. F.; Thompson, L. K.; Xu, Z. Strong Supramolecular-Based Magnetic Exchange in π -Stacked Radicals. Structure and Magnetism of a Hydrogen-Bonded Verdazyl Radical: Hydroquinone Molecular Solid. *J. Am. Chem. Soc.* **2001**, 123 (29), 7154–7159. <https://doi.org/10.1021/ja010725i>.
- (23) Hicks, R. *Stable Radicals: Fundamentals and Applied Aspects of Odd-Electron Compounds*; John Wiley & Sons, 2011.
- (24) Power, P. P. Persistent and Stable Radicals of the Heavier Main Group Elements and Related Species. *Chem. Rev.* **2003**, 103 (3), 789–809. <https://doi.org/10.1021/cr020406p>.
- (25) Norel, L.; Chamoreau, L.-M.; Journaux, Y.; Oms, O.; Chastanet, G.; Train, C. Verdazyl-Lanthanide (III) One Dimensional Compounds: Synthesis, Structure and Magnetic Properties. *Chem. Commun.* **2009**, No. 17, 2381–2383.
- (26) Caneschi, A.; Gatteschi, D.; Rey, P. The Chemistry and Magnetic Properties of Metal Nitronyl Nitroxide Complexes. *Prog. Inorg. Chem.* **1991**, 331–429.
- (27) McKinnon, S. D. J.; Patrick, B. O.; Lever, A. B. P.; Hicks, R. G. Electronic Structure Investigations of Neutral and Charged Ruthenium Bis(β -Diketonate) Complexes of Redox-Active Verdazyl Radicals. *J. Am. Chem. Soc.* **2011**, 133 (34), 13587–13603. <https://doi.org/10.1021/ja204575u>.
- (28) Hicks, R. G.; Koivisto, B. D.; Lemaire, M. T. Synthesis of Multitopic Verdazyl Radical Ligands. Paramagnetic Supramolecular Synthons. *Org. Lett.* **2004**, 6 (12), 1887–1890. <https://doi.org/10.1021/ol049746i>.
- (29) Johnston, C. W.; McKinnon, S. D. J.; Patrick, B. O.; Hicks, R. G. The First “Kuhn Verdazyl” Ligand and Comparative Studies of Its PdCl₂ Complex with Analogous 6-Oxoverdazyl Ligands. *Dalt. Trans.* **2013**, 42 (48), 16829. <https://doi.org/10.1039/c3dt52191e>.
- (30) Gilroy, J. B.; Koivisto, B. D.; McDonald, R.; Ferguson, M. J.; Hicks, R. G. Magnetostructural Studies of Copper(I) Verdazyl Radical Complexes. *J. Mater. Chem.* **2006**, 16 (26), 2618. <https://doi.org/10.1039/b603624d>.
- (31) Berry, D. E.; Hicks, R. G.; Gilroy, J. B. The Chemistry of Formazan Dyes. Synthesis and Characterization of a Stable Verdazyl Radical and a Related Boron-Containing Heterocycle. *J. Chem. Educ.* **2009**, 86 (1), 76. <https://doi.org/10.1021/ed086p76>.
- (32) Gilroy, J. B.; Ferguson, M. J.; McDonald, R.; Patrick, B. O.; Hicks, R. G. Formazans as β -Diketiminato Analogues. Structural Characterization of Boratetetrazines and Their Reduction to Borataverdazyl Radical Anions. *Chem. Commun.* **2007**, 412 (2), 126–128. <https://doi.org/10.1039/B609365E>.
- (33) Jornet, J.; Deumal, M.; Ribas-Ariño, J.; Bearpark, M. J.; Robb, M. A.; Hicks, R. G.; Novoa, J. J. Direct versus Mediated Through-Space Magnetic Interactions: A First Principles, Bottom-up Reinvestigation of the Magnetism of the Pyridyl-Verdazyl:Hydroquinone Molecular Co-Crystal. *Chem. - A Eur. J.* **2006**, 12 (15), 3995–4005. <https://doi.org/10.1002/chem.200501182>.
- (34) Kumar, V.; Shova, S.; Maurel, V.; Novitchi, G.; Train, C. Crystallographic Insights into the Synthesis

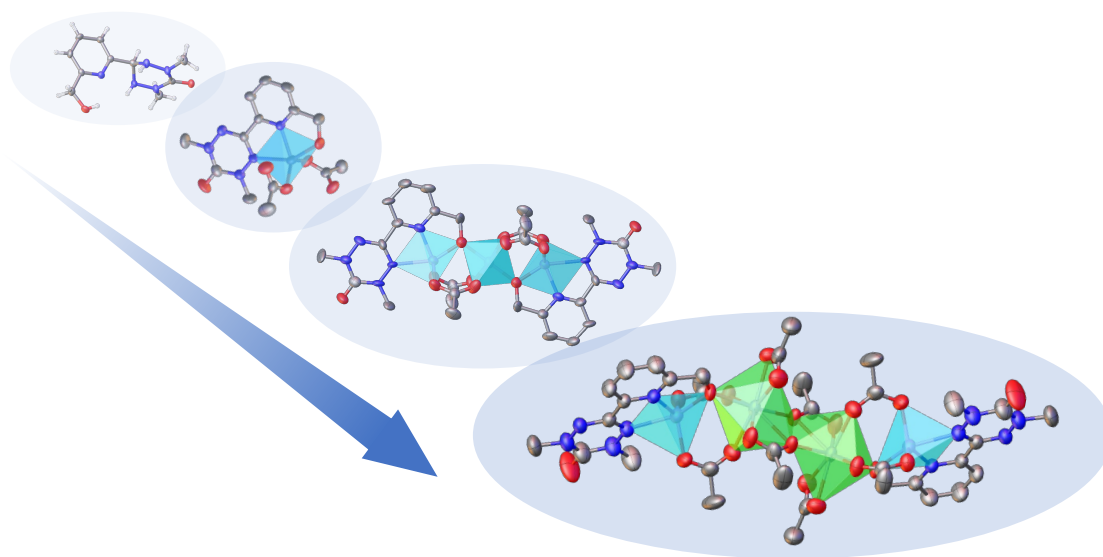
- and Magnetic Properties of Oxoverdazyl Radicals Functionalized by Benzoic Acid. *Eur. J. Inorg. Chem.* **2018**, 2018 (3), 517–524. <https://doi.org/10.1002/ejic.201700950>.
- (35) Kamebuchi, H.; Okubo, M.; Okazawa, A.; Enomoto, M.; Harada, J.; Ogawa, K.; Maruta, G.; Takeda, S.; Kojima, N.; Train, C. A Tricky Water Molecule Coordinated to a Verdazyl Radical-Iron (II) Complex: A Multitechnique Approach. *Phys. Chem. Chem. Phys.* **2014**, 16 (19), 9086–9095.
- (36) Gilroy, J. B.; Lemaire, M. T.; Patrick, B. O.; Hicks, R. G. Structure and Magnetism of a Verdazyl Radical Clathrate Hydrate. Strong Intermolecular Magnetic Interactions Derived from π -Stacking within Ice-like Channels. *CrystEngComm* **2009**, 11 (10), 2180–2184. <https://doi.org/10.1039/b908520c>.
- (37) Brook, D. J. R.; Fornell, S.; Stevens, J. E.; Noll, B.; Koch, T. H.; Eisfeld, W. Coordination Chemistry of Verdazyl Radicals: Group 12 Metal (Zn, Cd, Hg) Complexes of 1,4,5,6-Tetrahydro-2,4-Dimethyl-6-(2'-Pyridyl)-1,2,4,5-Tetrazin-3(2H)-One (PvdH3) and 1,5-Dimethyl-3-(2'-Pyridyl)-6-Oxoverdazyl (Pvd). *Inorg. Chem.* **2000**, 39 (3), 562–567. <https://doi.org/10.1021/ic9903883>.
- (38) Hicks, R. G.; Lemaire, M. T.; Thompson, L. K.; Barclay, T. M. Strong Ferromagnetic and Antiferromagnetic Exchange Coupling between Transition Metals and Coordinated Verdazyl Radicals. *J. Am. Chem. Soc.* **2000**, 122 (33), 8077–8078. <https://doi.org/10.1021/ja001627k>.
- (39) Pointillart, F.; Train, C.; Herson, P.; Michel, V. Verdazyl-Based Extended Structures: Synthesis, Structures and Magnetic Properties of Silver(I) One Dimensional Compounds. *New J. Chem. - NEW J CHEM* **2007**, 31. <https://doi.org/10.1039/b701686g>.
- (40) Oms, O.; Norel, L.; Chamoreau, L.-M.; Rousselière, H.; Train, C. Conformation and Crystal Packing Sensitivity to Substitution of Thioxo- and Oxo-Tetrazane Derivatives. *New J. Chem.* **2009**, 33 (8), 1663–1672. <https://doi.org/10.1039/B902225B>.
- (41) Plater, M. J.; Sinclair, J. P.; Kemp, S.; Gelbrich, T.; Hursthouse, M. B.; Gómez-garcía, C. J. New Tetrahydro-1,2,4,5-Tetrazinan-3-Ones and Oxoverdazyl Free Radicals PAPER : 05 / 3754. 1 (2), 515–520.
- (42) Liu, W.; Thorp, H. H. Bond Valence Sum Analysis of Metal-Ligand Bond Lengths in Metalloenzymes and Model Complexes. 2. Refined Distances and Other Enzymes. *Inorg. Chem.* **1993**, 32 (19), 4102–4105.
- (43) O'Keefe, M.; Brese, N. E. Atom Sizes and Bond Lengths in Molecules and Crystals. *J. Am. Chem. Soc.* **1991**, 113 (9), 3226–3229.
- (44) Brese, N. E.; O'keeffe, M. Bond-valence Parameters for Solids. *Acta Crystallogr. Sect. B* **1991**, 47 (2), 192–197.
- (45) Norel, L.; Chamoreau, L.-M.; Train, C. Modulation of Intermolecular Exchange Interaction in Organic Radical Based Compounds: Magneto-Structural Analysis of Phenol and Imidazolium Substituted Oxoverdazyl Radicals. *Polyhedron* **2010**, 29 (1), 342–348.
- (46) Koivisto, B. D.; Ichimura, A. S.; McDonald, R.; Lemaire, M. T.; Thompson, L. K.; Hicks, R. G. Intramolecular π -Dimerization in a 1,1'-Bis (Verdazyl) Ferrocene Diradical. *J. Am. Chem. Soc.* **2006**, 128 (3), 690–691.
- (47) Rota, J. B.; Guennic, B. Le; Robert, V. Toward Verdazyl Radical-Based Materials: Ab Initio Inspection of Potential Organic Candidates for Spin-Crossover Phenomenon. *Inorg. Chem.* **2010**, 49 (3), 1230–1237. <https://doi.org/10.1021/ic902197f>.
- (48) Rota, J.-B.; Norel, L.; Train, C.; Amor, N. Ben; Maynau, D.; Robert, V. Inspection of the Duality of a Verdazyl-Based Radical in Transition Metal Complexes: A II^* Donor Ligand and a Magnetic Partner. *J. Am. Chem. Soc.* **2008**, 130 (31), 10380–10385. <https://doi.org/10.1021/ja802027u>.
- (49) Hall, J. W.; Marsh, W. E.; Weller, R. R.; Hatfield, W. E. Exchange Coupling in the Alternating-Chain Compounds Catena-Di- μ -Chloro-Bis(4-Methylpyridine)Copper(II), Catena-Di- μ -Bromobis(N-Methylimidazole)Copper(II), Catena-[Hexanedione]Bis(Thiosemicarbazonato)]Copper(II), and Catena-[Octanedione Bis (Thiosem. *Inorg. Chem.* **1981**, 20 (4), 1033–1037. <https://doi.org/10.1021/ic50218a017>.
- (50) Hatfield, W. E. New Magnetic and Structural Results for Uniformly Spaced, Alternatingly Spaced, and Ladder-like Copper (II) Linear Chain Compounds (Invited). *J. Appl. Phys.* **1981**, 52 (3), 1985–1990. <https://doi.org/10.1063/1.329592>.

- (51) Lemaire, M. T.; Barclay, T. M.; Thompson, L. K.; Hicks, R. G. Synthesis, Structure, and Magnetism of a Binuclear Co(II) Complex of a Potentially Bis-Tridentate Verdazyl Radical Ligand. *Inorganica Chim. Acta* **2006**, *359* (9), 2616–2621. <https://doi.org/10.1016/j.ica.2005.09.060>.
- (52) Kahn, O. *Molecular Magnetism*; 1993. <https://doi.org/10.1039/b612962p>.
- (53) Titiš, J.; Boča, R. Magnetostructural D Correlations in Hexacoordinated Cobalt(II) Complexes. *Inorg. Chem.* **2011**, *50* (22), 11838–11845. <https://doi.org/10.1021/ic202108j>.
- (54) Titiš, J.; Hudák, J.; Kožíšek, J.; Krutošíková, A.; Moncol', J.; Tarabová, D.; Boča, R. Structural, Spectral and Magnetic Properties of Carboxylato Cobalt(II) Complexes with Heterocyclic N-Donor Ligands: Reconstruction of Magnetic Parameters from Electronic Spectra. *Inorganica Chim. Acta* **2012**, *388*, 106–113. <https://doi.org/10.1016/j.ica.2012.03.036>.
- (55) Papánková, B.; Boča, R.; Dlháň, L.; Nemeč, I.; Titiš, J.; Svoboda, I.; Fuess, H. Magneto-Structural Relationships for a Mononuclear Co(II) Complex with Large Zero-Field Splitting. *Inorganica Chim. Acta* **2010**, *363* (1), 147–156. <https://doi.org/10.1016/j.ica.2009.09.028>.
- (56) Rajnáč, C.; Titiš, J.; Boča, R.; Moncol', J.; Padělková, Z. Self-Assembled Cobalt(II) Schiff Base Complex: Synthesis, Structure, and Magnetic Properties. *Monatshfte für Chemie - Chem. Mon.* **2011**, *142* (8), 789–795. <https://doi.org/10.1007/s00706-011-0521-7>.
- (57) Schweinfurth, D.; Krzystek, J.; Atanasov, M.; Klein, J.; Hohloch, S.; Telsler, J.; Demeshko, S.; Meyer, F.; Neese, F.; Sarkar, B. Tuning Magnetic Anisotropy Through Ligand Substitution in Five-Coordinate Co(II) Complexes. *Inorg. Chem.* **2017**, *56* (9), 5253–5265. <https://doi.org/10.1021/acs.inorgchem.7b00371>.
- (58) Schweinfurth, D.; Sommer, M. G.; Atanasov, M.; Demeshko, S.; Hohloch, S.; Meyer, F.; Neese, F.; Sarkar, B. The Ligand Field of the Azido Ligand: Insights into Bonding Parameters and Magnetic Anisotropy in a Co(I)-Azido Complex. *J. Am. Chem. Soc.* **2015**, *137* (5), 1993–2005. <https://doi.org/10.1021/ja512232f>.
- (59) Woods, T. J.; Ballesteros-Rivas, M. F.; Gómez-Coca, S.; Ruiz, E.; Dunbar, K. R. Relaxation Dynamics of Identical Trigonal Bipyramidal Cobalt Molecules with Different Local Symmetries and Packing Arrangements: Magnetostructural Correlations and Ab Initio Calculations. *J. Am. Chem. Soc.* **2016**, *138* (50), 16407–16416. <https://doi.org/10.1021/jacs.6b10154>.
- (60) Rajnáč, C.; Titiš, J.; Šalitroš, I.; Boča, R.; Fuhr, O.; Ruben, M. Zero-Field Splitting in Pentacoordinate Co(II) Complexes. *Polyhedron* **2013**, *65*, 122–128. <https://doi.org/10.1016/j.poly.2013.08.029>.
- (61) Ruamps, R.; Batchelor, L. J.; Guillot, R.; Zakhia, G.; Barra, A. L.; Wernsdorfer, W.; Guihery, N.; Mallah, T. Ising-Type Magnetic Anisotropy and Single Molecule Magnet Behaviour in Mononuclear Trigonal Bipyramidal Co(II) Complexes. *Chem. Sci.* **2014**, *5*, 3418.
- (62) Mondal, A. K.; Goswami, T.; Misra, A.; Konar, S. Probing the Effects of Ligand Field and Coordination Geometry on Magnetic Anisotropy of Pentacoordinate Cobalt(II) Single-Ion Magnets. *Inorg. Chem.* **2017**, *56* (12), 6870–6878. <https://doi.org/10.1021/acs.inorgchem.7b00233>.
- (63) Gransbury, G. K.; Boulon, M. E.; Mole, R. A.; Gable, R. W.; Moubaraki, B.; Murray, K. S.; Sorace, L.; Soncini, A.; Boskovic, C. Single-Ion Anisotropy and Exchange Coupling in Cobalt(I)-Radical Complexes: Insights from Magnetic and: Ab Initio Studies. *Chem. Sci.* **2019**, *10* (38), 8855–8871. <https://doi.org/10.1039/c9sc00914k>.
- (64) Caneschi, A.; Gatteschi, D.; Lalioti, N.; Sessoli, R.; Sorace, L.; Tangoulis, V.; Vindigni, A. Ising-Type Magnetic Anisotropy in a Cobalt(II) Nitronyl Nitroxide Compound: A Key to Understanding the Formation of Molecular Magnetic Nanowires. *Chem. - A Eur. J.* **2002**, *8* (1), 286–292. [https://doi.org/10.1002/1521-3765\(20020104\)8:1<286::AID-CHEM286>3.0.CO;2-D](https://doi.org/10.1002/1521-3765(20020104)8:1<286::AID-CHEM286>3.0.CO;2-D).
- (65) Maspoch, D.; Domingo, N.; Ruiz-Molina, D.; Wurst, K.; Hernández, J. M.; Lloret, F.; Tejada, J.; Rovira, C.; Veciana, J. First-Row Transition-Metal Complexes Based on a Carboxylate Polychlorotriphenylmethyl Radical: Trends in Metal-Radical Exchange Interactions. *Inorg. Chem.* **2007**, *46* (5), 1627–1633. <https://doi.org/10.1021/ic061815x>.
- (66) Caneschi, A.; Dei, A.; Gatteschi, D.; Tangoulis, V. Antiferromagnetic Coupling in a Six-Coordinate High Spin Cobalt(II)-Semiquinonato Complex. *Inorg. Chem.* **2002**, *41* (13), 3508–3512. <https://doi.org/10.1021/ic020243n>.

- (67) Dori, B. Z. V. I.; Gray, H. B.; Dori, Z.; Gray, H. B. High-Spin , Five-Coordinate Cobalt (II) Complexes. **1968**, 7 (5), 1966–1969.
- (68) Wood, J. S. Ligand Field Theory for Pentacoordinate Molecules. I. The Electronic Spectra of Species with D_{3h} and C_{3v} Symmetry. *Inorg. Chem.* **1968**, 7 (5), 852–859. <https://doi.org/10.1021/ic50063a002>.
- (69) Bertini, I.; Gatteschi, D.; Scozzafava, A. Ligand Field Interpretation of High-Spin Trigonal-Bipyramidal Cobalt(II) Complexes. *Inorg. Chem.* **1975**, 14 (4), 812–815. <https://doi.org/10.1021/ic50146a024>.
- (70) Morassi, R.; Bertini, I.; Sacconi, L. Five-Coordination in Iron(II); Cobalt(II) and Nickel(II) Complexes. *Coord. Chem. Rev.* **1973**, 11 (4), 343–402. [https://doi.org/10.1016/S0010-8545\(00\)80248-9](https://doi.org/10.1016/S0010-8545(00)80248-9).
- (71) Sacconi, L. Five-Coordination in 3d Metal Complexes. *Pure Appl. Chem.* **1968**, 17 (1), 95–128. <https://doi.org/10.1351/pac196817010095>.
- (72) Makinen, M. W.; Kuo, L. C.; Yim, M. B.; Wells, G. B.; Fukuyama, J. M.; Kim, J. E. Ground Term Splitting of High-Spin Cobalt(2+) Ion as a Probe of Coordination Structure. 1. Dependence of the Splitting on Coordination Geometry. *J. Am. Chem. Soc.* **1985**, 107 (18), 5245–5255. <https://doi.org/10.1021/ja00304a035>.
- (73) Palii, A.; Tsukerblat, B.; Klokishner, S.; Dunbar, K. R.; Clemente-Juan, J. M.; Coronado, E. Beyond the Spin Model: Exchange Coupling in Molecular Magnets with Unquenched Orbital Angular Momenta. *Chem. Soc. Rev.* **2011**, 40 (6), 3130. <https://doi.org/10.1039/c0cs00175a>.
- (74) Palii, A.; Tsukerblat, B.; Clemente-Juan, J. M.; Coronado, E. Magnetic Exchange between Metal Ions with Unquenched Orbital Angular Momenta: Basic Concepts and Relevance to Molecular Magnetism. *Int. Rev. Phys. Chem.* **2010**, 29 (1), 135–230. <https://doi.org/10.1080/01442350903435256>.
- (75) Clemente-Juan, J. M.; Coronado, E. Magnetic Clusters from Polyoxometalate Complexes. *Coord. Chem. Rev.* **1999**, 193–195, 361–394. [https://doi.org/10.1016/S0010-8545\(99\)00170-8](https://doi.org/10.1016/S0010-8545(99)00170-8).
- (76) Andres, H.; Aebersold, M.; Gudel, H. U.; Clemente, J. M.; Coronado, E.; Buttner, H.; Kearly, G.; Zolliker, M. Anisotropic Exchange Coupling in the Keggin Derivative K-8[Co-2(D2o)(W11o39)]Center Dot Nd(2)O. *Chem. Phys. Lett.* **1998**, 289 (3–4), 224–230.
- (77) Andres, H.; Clemente-Juan, J. M.; Aebersold, M.; Güdel, H. U.; Coronado, E.; Büttner, H.; Kearly, G.; Melero, J.; Burriel, R. Magnetic Excitations in Polyoxometalate Clusters Observed by Inelastic Neutron Scattering: Evidence for Anisotropic Ferromagnetic Exchange Interactions in the Tetrameric Cobalt(II) Cluster [Co4(H2O)2(PW9O34)2]10-. Comparison with the Magnetic and Specific. *J. Am. Chem. Soc.* **1999**, 121 (43), 10028–10034. <https://doi.org/10.1021/ja990198r>.
- (78) Clemente-Juan, J. M.; Andres, H.; Borrás-Almenar, J. J.; Coronado, E.; Güdel, H. U.; Aebersold, M.; Kearly, G.; Buttner, H.; Zolliker, M. Magnetic Excitations in Polyoxometalate Clusters Observed by Inelastic Neutron Scattering: Evidence for Ferromagnetic Exchange Interactions and Spin Anisotropy in the Tetrameric Nickel(II) Cluster [Ni4(H2O)2(PW9O34)2]10- and Comparison with the Magnetic P. *J. Am. Chem. Soc.* **1999**, 121 (43), 10021–10027. <https://doi.org/10.1021/ja990197z>.
- (79) Palii, A. V.; Tsukerblat, B. S.; Coronado, E.; Clemente-Juan, J. M.; Borrás-Almenar, J. J. Microscopic Approach to the Pseudo-Spin-1/2 Hamiltonian for Kramers Doublets in Exchange Coupled Co(II) Pairs. *Inorg. Chem.* **2003**, 42 (7), 2455–2458. <https://doi.org/10.1021/ic0259686>.
- (80) Caneschi, A.; Gatteschi, D.; Lalioti, N.; Sangregorio, C.; Sessoli, R.; Venturi, G.; Vindigni, A.; Rettori, A.; Pini, M. G.; Novak, M. A. Cobalt(II)-Nitronyl Nitroxide Chains as Molecular Magnetic Nanowires. *Angew. Chemie - Int. Ed.* **2001**, 40 (9), 1760–1763. [https://doi.org/10.1002/1521-3773\(20010504\)40:9<1760::AID-ANIE1760>3.0.CO;2-U](https://doi.org/10.1002/1521-3773(20010504)40:9<1760::AID-ANIE1760>3.0.CO;2-U).
- (81) Palii, A. V.; Tsukerblat, B. S.; Coronado, E.; Clemente-Juan, J. M.; Borrás-Almenar, J. J. Orbitally Dependent Magnetic Coupling between Cobalt(II) Ions: The Problem of the Magnetic Anisotropy. *J. Chem. Phys.* **2003**, 118 (12), 5566–5581. <https://doi.org/10.1063/1.1555122>.
- (82) Dolomanov, O. V.; Bourhis, L. J.; Gildea, R. J.; Howard, J. A. K.; Puschmann, H. OLEX2 : A Complete Structure Solution, Refinement and Analysis Program. *J. Appl. Crystallogr.* **2009**, 42 (2), 339–341. <https://doi.org/10.1107/S0021889808042726>.
- (83) Sheldrick, G. M. Crystal Structure Refinement with SHELXL. *Acta Crystallogr. Sect. C Struct. Chem.* **2015**, 71 (Md), 3–8. <https://doi.org/10.1107/S2053229614024218>.

- (84) Pascal, P. Recherches Magnetochimiques. *Ann. Chim. Phys.* **1910**, *19*, 5–70.
- (85) Chilton, N. F.; Anderson, R. P.; Turner, L. D.; Soncini, A.; Murray, K. S. PHI: A Powerful New Program for the Analysis of Anisotropic Monomeric and Exchange-Coupled Polynuclear d- and f-Block Complexes. *J. Comput. Chem.* **2013**, *34* (13), 1164–1175. <https://doi.org/10.1002/jcc.23234>.

TOC Graphic



Self-assembly in solution going from verdazyl (vd) radicals to 2p-3d and 2p-3d-4f clusters. The cobalt(II) centers definitely convey strong magnetic anisotropy but do not lead to Single-Molecules Magnets properties as observed in the vd-Co(II)-Dy(III) analog (*Inorg. Chem.* 2016, *55*, 12122)